



Author: Chrimes, Adam F.; Khoshmanesh, Khashayar; Stoddart, Paul R.; Mitchell, Arnan; Kalantar-zadeh, Kourosh  
Title: Microfluidics and Raman microscopy: current applications and future challenges  
Year: 2013  
Journal: Chemical Society Reviews  
Volume: 42  
Issue: 13  
Pages: 5880-5906  
URL: <http://dx.doi.org/10.1039/C3CS35515B>

Copyright: Copyright © The Royal Society of Chemistry 2013. The accepted manuscript is made available in accordance with the copyright policy of the publisher.

This is the author's version of the work, posted here with the permission of the publisher for your personal use. No further distribution is permitted. You may also be able to access the published version from your library.

The definitive version is available at: <http://dx.doi.org/10.1039/C3CS35515B>

Cite this: DOI: 10.1039/C3CS35515B

www.rsc.org/csr

CRITICAL REVIEW

# Microfluidics and Raman microscopy: current applications and future challenges

Adam F. Chrimes,<sup>\*a</sup> Khashayar Khoshmanesh,<sup>a</sup> Paul R. Stoddart,<sup>b</sup> Arnan Mitchell,<sup>a</sup> and Kourosh Kalantar-zadeh<sup>a</sup>

<sup>5</sup> Received (in XXX, XXX) Xth XXXXXXXXXX 20XX, Accepted Xth XXXXXXXXXX 20XX

DOI: 10.1039/C3CS35515B

Raman microscopy systems are becoming increasingly widespread and accessible for characterising chemical species. Microfluidic systems are also progressively finding their way into real world applications. Therefore, it is anticipated that the integration of Raman systems with microfluidics will become increasingly attractive and practical. This review aims to provide an overview of Raman microscopy-microfluidics integrated systems for researchers who are actively interested in utilising these tools. The fundamental principles and application strengths of Raman microscopy are discussed in the context of microfluidics. Various configurations of microfluidics that incorporate Raman microscopy methods are presented, with applications highlighted. Data analysis methods are discussed, with a focus on assisting the interpretation of Raman-microfluidics data from complex samples. Finally, possible future directions of Raman-microfluidic systems are presented.

## 1. Introduction

Microfluidics, which deals with geometrically constrained small volume fluids, allows for the flexible and highly controlled manipulation of liquids, suspended particles and biological samples. It is also well-known that Raman microscopy is a powerful tool that can provide unparalleled insight into the organic and inorganic chemical components and biomaterials at low sample volumes. Combining Raman microscopy with microfluidics allows for the accurate monitoring, detection and analysis of a wide range of samples in microfluidic environments.

The Raman phenomenon was first discovered by Sir Chandrasekhara V. Raman in the 1920s,<sup>1</sup> and since then, progress has been made in understanding the mechanisms and theoretical descriptions of the effect. Raman spectroscopy is particularly suited for analytical chemistry, given that it is generally non-destructive, requires little or no sample preparation, offers high discrimination between sample components and is capable of studying gaseous, aqueous and solid samples.<sup>2-5</sup>

Raman microscopy is an advanced spectroscopic technique, incorporating optical microscopes, excitation lasers, optical filtering and manipulation devices, and spectrometers. The Raman microscope offers the advantages of high spatial resolution and optical sensitivity, due to the increased photon flux from the highly focused laser source and high collection efficiency of the objective lens. By providing specific information about the vibrational energy levels of chemical bonds and molecules, Raman microscopy is an invaluable tool for 'fingerprinting' materials, and is finding increasing applications in medicine, biotechnology, material sciences and even forensics.<sup>6-9</sup>

The field of microfluidics emerged in the early 1980s and it is now routinely used in a variety of commercial applications including inkjet print-heads, lab-on-a-chip (LOC) systems, deoxyribonucleic acid (DNA) chips, and micro-thermal cooling devices to name just a few. Of particular interest to this review are the microfluidic systems that allow for precise manipulation of fluids that are geometrically constrained to small volumes, in the order of micro- and pico-litres.<sup>10,11</sup>

Microfluidic systems are becoming increasingly attractive in chemistry and biochemistry, as they allow for the miniaturisation of systems that are normally employed in those laboratories. Microfluidic systems are also useful tools for the handling of fluids and suspended materials. As such, they improve the efficiency of procedures by enhancing material mobility and vastly reducing required sample volumes. Advances in microfluidics have resulted in the creation of many innovative technologies in molecular biology processes, proteomics and DNA analysis.<sup>11-14</sup>

Microfluidic platforms that integrate optical and spectroscopic analysis, exploiting both absorption and scattering techniques, have been extensively reported.<sup>15,16</sup> Different types of spectroscopy systems have been used with microfluidics, including ultraviolet visible absorption (UV-Vis), Fourier transform infrared spectroscopy (FTIR), fluorescence spectroscopy and Raman spectroscopy (inelastic scattering). Amongst these techniques, Raman spectroscopy has proven to be highly compatible with microfluidics. Driven by improvements in hardware, the technique has largely overcome the concern that it is a "weak effect", as Raman scattering signal intensities are much smaller than those obtained by other spectroscopic methods.<sup>17</sup> When dealing with low volume samples, and possibly

low concentration analytes, Raman microscopy provides sub-micron spatial resolution with very high sensitivity and selectivity for microfluidic systems. Raman microscopy can also provide information regarding target materials very rapidly, with latencies measured in the order of seconds, or even fractions of a second, allowing for real-time monitoring processes to be practically considered in such systems.

Integrated Raman microscopy and microfluidic systems (“Raman-microfluidics”) have already found a plethora of applications in the analysis of materials from low volume liquid media, especially when samples are rare and expensive (medical samples; forensic traces and pharmaceuticals), in microreactors for which constant monitoring is required (pre-processing of biochemical samples and tissue engineering) and monitoring of environmental samples (water quality and biosensing). This track record suggests that the integration of Raman microscopy as a powerful analytical tool, along with the unique properties of microfluidics, will be a key enabler for many future applications.

Many reports on Raman microscopy-microfluidics integration exist. However, a comprehensive review on Raman microscopy in microfluidic environments is currently lacking. This review aims to provide the reader with a detailed understanding of the capabilities of such systems and the opportunities and challenges they present. The article has been designed to be informative for a broad range of specialists, including those in the fields of microfluidics, vibrational spectroscopy, optics, biotechnology, biochemistry, chemistry and analytical chemistry who seek to exploit Raman-microfluidic systems for their diverse applications.

## 2. Raman microscopy methods

To better understand the specific capabilities and limitations of Raman microscopy-microfluidics, this section presents an overview of the instrumentation and critical parameters, on a number of variations on Raman microscopy, and then discusses the opportunities and challenges of each of these in the context of microfluidic devices.

### 2.1 Instrumentation and critical parameters

The Raman effect takes place when light illuminates a region, interacting with the molecules that are present in this region. The incident photons do not have sufficient energy to excite a quantum transition from one stable electron configuration to another, but the photon interaction does perturb the electron configuration of the molecule to an unstable ‘virtual’ state during photon scattering. Most commonly, these scattered photons have the same energy, (and therefore frequency and wavelength) as that of the incident photon. However, a small fraction of photons (on the order of 1 in  $10^6$ ) are scattered with a change in energy (and hence frequency). The difference can be attributed to energy gained or lost to vibrational energy in the molecule. As such, the photon energy can be shifted to lower or higher frequencies depending on whether they lose or gain energy. These shifts in frequency are called Stokes and anti-Stokes shifts, respectively. For molecules to exhibit the Raman effect they must have non-zero polarisability, that is to say that an incident photon must be able to effectively deform the electron configuration of the molecule. The degree of this deformation determines the Raman

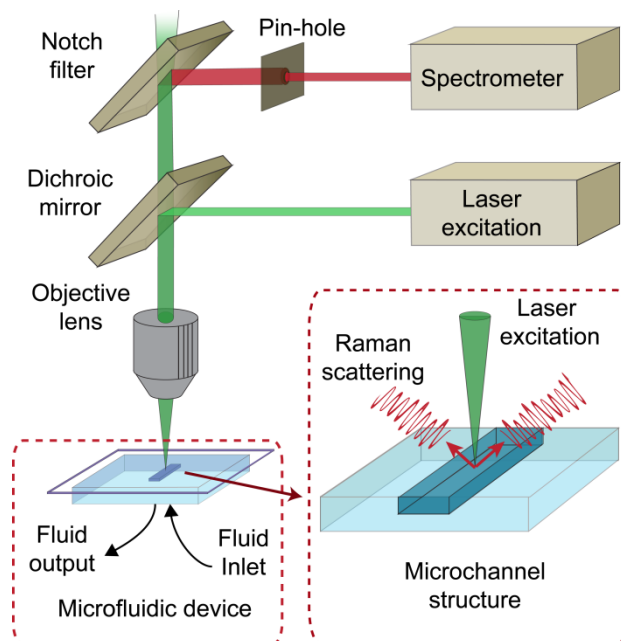


Fig. 1 Schematic diagram of a confocal Raman system integrated with a microfluidic unit

scattering intensity, due to resonant interactions with the rotational and vibrational states of the molecule.

Raman-microfluidic systems can interrogate materials suspended in liquid media or at the interfaces with liquids. Many types of liquids have distinct Raman signatures, allowing them to be identified, as well as recognition of mixtures of different liquid types. Solid suspensions and dissolved gases can be differentiated using Raman measurements in microfluidic environments. Additionally, Raman microscopy systems are one of the best tools for understanding the properties of solid/liquid interfaces as the excitation beam can be tightly focused at the interface.

In Raman-microfluidic microscopy, a laser beam is focussed into the microfluidic environment through the use of a microscope objective lens. The lens also collects the light, which is backscattered from the sample, and passes it to the spectrometer via a dichroic (color separating) filter. Before entering the spectrometer, the strong elastically scattered Rayleigh wavelength (with the same wavelength as the incident beam) is removed by the dichroic filter, while the in-elastic Raman components are passed. A conventional Raman microscopy system is shown in Fig. 1, which is comprised of a dichroic filter and a pin-hole with a controllable diameter to ensure that only signals from the small volume at the focal point are collected. The spectrometer counts the intensity of light collected at various frequencies.

Raman spectroscopy allows for the integration with microscopic analysis techniques and is capable of collecting spectra from very small volumes ( $< 1 \mu\text{l}$ ), making it suitable for analysis on the microfluidics size scale. Raman microscopy can approach very high spatial resolutions. For example, using a 633 nm laser source with a pinhole of 50  $\mu\text{m}$  in radius and a  $60\times/1.2$  numerical aperture (NA) objective, lateral and depth resolutions of approximately 0.25 and 1.7  $\mu\text{m}$ , respectively, can be achieved. These dimensions are comparable to features that can readily be realised in microfluidic systems.

The unit for Raman spectroscopy is the wavenumber, which is the reciprocal of the wavelength shift relative to the laser wavelength, expressed as  $1/\Delta\lambda$  with units of  $\text{cm}^{-1}$ . Raman shifts in the range 10–400  $\text{cm}^{-1}$  can be used to study the rotational aspect of molecular bonds, whereas the range 400–4000  $\text{cm}^{-1}$  contains vibrations associated with vibrational-rotational structures. For organic molecules the range from 500–2000  $\text{cm}^{-1}$  is known as the ‘fingerprint’ region.

## 2.2 Variations of Raman spectroscopy

Raman spectra are inherently weak due to the rarity of the inelastic scattering phenomenon. Thus, much effort has been invested to design Raman systems with enhanced sensitivity and spectral resolution. Each enhancement technique comes at the cost of some specific trade off. The following presents some of the key Raman spectroscopic variations and discusses their relative advantages and limitations for microfluidic devices.

### 2.2.1 Surface-enhanced Raman spectroscopy

Surface-enhanced Raman spectroscopy (SERS) was first observed by Fleischmann *et al.*<sup>18</sup> The effect originates from nanocolloids of metals, such as silver or gold, which generate localised surface plasmon resonances when excited by a laser source. These plasmonic effects can be observed in nanostructured surfaces of such metals as well. The existence of plasmon fields enhance the intensity of the Raman signals from chemicals within their range, with enhancements as high as  $10^8$  reported for well optimised systems.<sup>19</sup> Although the fundamental electromagnetic basis of SERS is now well established, surface enhancement has also been associated with charge transfer effects in the metal-adsorbate system (chemical enhancements).<sup>20,21</sup> A large number of excellent reviews, describing SERS and its principles are already available.<sup>21–24</sup> Access to a variety of commercially available colloidal suspensions makes SERS suitable for microfluidics and has been demonstrated for measuring many low concentration analytes such as 4-aminobenzenethiol,<sup>25</sup> Rhodamine 6G<sup>26</sup> and crystal violet<sup>27</sup> from inside microfluidic devices. While extraordinary enhancement, to the point of single molecule detection, has been demonstrated, it is crucial that the analyte be in close proximity to and in the correct orientation relative to the metal nanostructures, limiting the technique to analysis of chemicals that can be effectively immobilised on the nanostructured metal surface. Whether that surface is a fixed structure or nanocolloid does not change this requirement. Altogether, there are many examples which integrate microfluidics with confocal SERS systems. Microfluidics are used in creating small volume/high concentration samples for obtaining detailed spectroscopic analytical information from the target materials.<sup>28</sup> Microfluidics are used as to control the mixing between nanometals and the target analytes prior to SERS measurements,<sup>29</sup> and also provide solutions in controlling the spacing between nanoparticles to enhance the SERS signal.<sup>30</sup> For more information refer to reviews on SERS and microfluidics.<sup>31,32</sup>

### 2.2.2 Resonance Raman spectroscopy

Resonance Raman spectroscopy (RRS) tunes the laser illumination wavelength close to one of the electronic transitions of the target molecule, leading to an enhancement of the Raman scattering intensity from the vibrational modes associated with the electronic transition, known as the Franck-Condon active

modes.<sup>33</sup> Lines due to other vibrational modes are also present in the Raman spectrum, however these are not enhanced. This method is capable of distinguishing Raman peak shifts of specific bonds in large organic molecules, such as chromophores,<sup>34</sup> which would otherwise show complex Raman signatures in the spectral region of interest.<sup>35</sup> This method relies on tuneable lasers for the Raman excitation, which are readily available, but often with limited power. Confocal techniques have been shown to direct the excitation beam onto specific locations of a target analyte within a microfluidic system, thereby compensating for such power limitations.<sup>36</sup>

### 2.2.3 Surface-enhanced resonance Raman spectroscopy

Resonance Raman spectroscopy can be enhanced further through combination with SERS to form surface-enhanced resonance Raman spectroscopy (SERRS). This combination allows the study of specific bonds from extremely small sample volumes compatible with microfluidics dimensions.<sup>37–39</sup> SERRS can be readily implemented in microfluidic systems by introducing nanostructured metal surfaces or particles, enabling identification and analysis of large proteins and other macro molecules such as oligonucleotides<sup>37</sup> and trinitrotoluene.<sup>40</sup>

### 2.2.4 Coherent anti-Stokes Raman spectroscopy

In Coherent anti-Stokes Raman spectroscopy (CARS), two pulsed laser beams, known as pump and probe beams, are used to generate an enhanced anti-Stokes photon. This method has been proven for specific samples to be far more sensitive than traditional Raman microscopy, and is gaining recognition in the scientific community.<sup>41–43</sup> CARS microscopy has been particularly effective in monitoring the structure and local environment of lipids and water molecules, which may be useful for specialised applications in microfluidics.<sup>44</sup> However, CARS is a non-linear optical effect that relies on the exceptionally high peak power possible with ultra-short pulses. Dispersion must be carefully managed to maintain such high pulse powers and the pulse and probe must be carefully synchronised placing constraints on the geometry and stability of the optical interface to the microfluidic platform. Further, the intense pulses can cause multi-photon absorption leading to strong fluorescence, or damage in materials such as polymers or organic matter. This constrains the choice of materials for interrogation windows or analytes which can be probed in microfluidic systems.

### 2.2.5 Stimulated Raman scattering

Stimulated Raman scattering (SRS) microscopy is similar to CARS in that pump and probe beams are used to make the molecular bonds oscillate in phase, while actively pumping the vibrational states, leading to significant enhancement of the Raman signal. The key difference for SRS, as compared to CARS, is that the probe beam is at the Stokes wavelength. The intensity of the scattered light at the pump wavelength experiences a stimulated Raman loss (SRL), while the intensity of the scattered light at the Stokes wavelength experiences a stimulated Raman gain (SRG). SRS microscopy has a major advantage over CARS in that it provides low-background imaging with improved chemical contrast,<sup>45</sup> both of which are potentially important for microfluidics where water is often the major source of non-resonant background signal in the sample. However, applications in microfluidics may once again be limited by dispersive broadening when passing through an optical window, limiting its applications in microfluidic systems for the

time being.

### 2.2.6 Tip-enhanced Raman spectroscopy

Atomically sharp metallic coated tips, such as those used in atomic force microscopy (AFM) machines, are used in tip-enhanced Raman spectroscopy (TERS). When coated with nanostructured, plasmonically active metals, these tips produce strong plasmon fields in their vicinity. Hence, TERS can have the spatial resolution as small as 10 nm, which has been demonstrated with single molecule sensitivity.<sup>46-48</sup> Furthermore, with the development of AFMs that operate in liquids, this technology has the potential to be incorporated into microfluidic devices for measurements at high spatial resolution.<sup>49</sup>

### 2.3 Considerations for Raman microscopy in microfluidics

Although Raman microscopy systems are relatively versatile, there are still some constraints that must be considered, stemming from the limitations of Raman microscopy and microfluidic systems, as well as their integration. Specifically, these challenges relate to the small volume of detection and how to manage the scattering process so as to optimise spectral collection efficiency. It is also important to minimise damage to samples and microfluidic devices due to the optical power levels generated by the Raman excitation systems. These issues are highlighted and discussed in more detail.

#### 2.3.1 Droplet surfaces

When imaging droplets (from inside microfluidic channels, placed on substrates or on the surface of open microchannels), the convex/concave shape of a droplet surface can adversely affect the Raman system's ability to accurately measure materials suspended in such droplets. This is partly due to the fact that there is a refractive index difference between the droplet and the air. Additionally, the shape of the droplet surface creates a lensing effect that distorts the focus and reduces the spatial resolution. Therefore, it is important to ensure that the Raman excitation enters the droplet through as flat a surface as possible, ideally through an optically transparent substrate, such as glass or quartz.<sup>50</sup> For open microfluidic channel designs, it is important to consider the width of the microchannel to ensure that the liquid is as flat as possible so as to minimise any issues caused by various distortions and chromatic aberration.<sup>51</sup>

#### 2.3.2 Focal length

As the microfluidic device walls and substrates can be several millimetres thick, the focal length must be long enough so as to penetrate inside the liquid media. Therefore the correct focal length is required to successfully integrate Raman microscopy and microfluidics. The focal length of a Raman system is determined by the optical arrangement of the microscope, but most importantly by the objective lens. Lower magnification objective lenses tend to have longer focal distances, generally making them more suitable for microfluidic systems. High magnification, long working distance objectives can also be used, at the expense of optical intensity and hence, reduced signal to noise ratio. Water and oil immersion objectives can also be considered. In some cases lenses are not necessary, specifically in the case of fibre based Raman systems, where the fibre is integrated with the microchannel and the tip of the fibre exposed to the target liquids.<sup>52</sup>

#### 2.3.3 Detection volume

Raman microscope systems focus the excitation beam into a

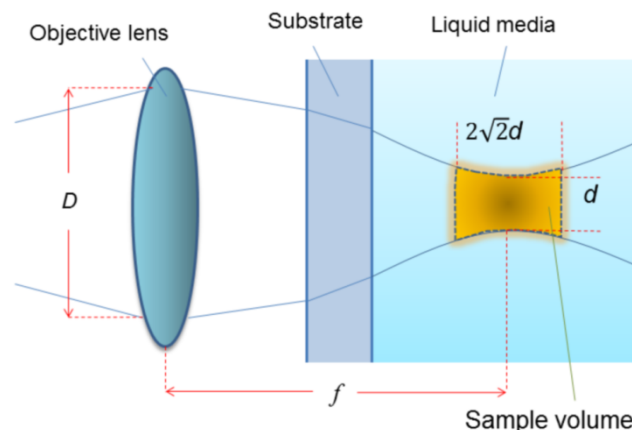


Fig. 2 Schematic of the optical system showing the definitions of spot size, depth of field, focal length and detection volume

small volume using an objective lens. The size of the detection area is dominated by the spot size, or diameter, of the excitation beam at the focal point (Fig. 2). This diameter ( $d$ ) is proportional to  $f$  the focal length of the lens and  $\lambda$  the wavelength of the laser source and it is inversely proportional to  $D$ , the lens diameter ( $d \propto f\lambda/D$ ). The other important parameter for the detection volume is the depth of focus. The depth of focus (also known as the confocal parameter) is generally estimated as twice the Rayleigh range (the distance between the  $\sqrt{2}d$  spot size points). The value can be approximated as  $\pi d^2/2\lambda$ . In order to achieve a small depth of focus the microscope must be operated in confocal mode, where the size of the spectrometer entrance slit is reduced to the smallest value compatible with the required signal throughput.

To integrate Raman and microfluidic measurements, the optimum spot size must be chosen, as the full focal volume is generally placed within the liquid medium to ensure that the Raman signals primarily arise from interactions with the target analytes. As mentioned previously, the use of high magnification microscope objectives for Raman spectroscopy tends to increase the signal to noise ratio and reduces the minimum detection limit by focusing the beam more tightly, and increasing the collection angle. Targeted detection is also possible in microfluidics using mechanical sample stages to move the targets with sub-micron spatial accuracy (e.g. piezoelectric stages).

#### 2.3.4 Excitation wavelength

The optimum choice of excitation laser wavelength is important for Raman spectroscopic applications in microfluidics. The intensity of Raman scattering scales inversely as the fourth power of the wavelength, so it is generally preferable to use shorter excitation wavelengths. However, issues arise when Raman microscopy of biological samples is required, because of the potential to produce large interfering fluorescence signals as the photon energy increases. The shot noise of the fluorescence signal can mask the desired Raman signatures of the samples.<sup>53</sup> The majority of biological samples are also strong absorbers of optical energy, particularly at shorter wavelengths (blue and UV). Modern Raman microscopes usually offer several different options for excitation wavelength, however for these systems the diffraction grating efficiency and detector sensitivity must also be taken into account for each operating wavelength.

For biological samples, the use of a typical excitation

wavelength of 532 nm can produce such fluorescent signals. One solution is to use longer wavelength lasers such as red, or near infrared, so that the photon energy is below the fluorescence excitation band. While this may reduce the fluorescence in the sample, it also reduces the Raman scattering efficiency of the system, requiring higher power lasers or longer integration times. Additionally, the choice of excitation wavelength is critical for resonance, and surface-enhanced resonance Raman scattering. While resonant wavelengths may be advantageous for detection at trace levels, other wavelengths may be preferred in situations where non-resonant bonds are of analytical interest.<sup>54,55</sup>

### 2.3.5 Optical power

In general, the scattering intensity can be increased simply by increasing the excitation power, but high power densities at the focal point can cause damage to thermally liable biological samples in the microfluidic environment. Additionally, high laser power at the focal point can cause localised turbulence or induce tweezing effects on nanocolloids in the microfluidics.<sup>56,57</sup> Therefore, the optical power for Raman excitation should be carefully optimised in each case to ensure that the sample is not damaged during the measurement. Much work has been done in determining the damage threshold for optical power applied to biological samples.<sup>57,58</sup>

Another strategy to reduce the potential damage to biological samples is to reduce the laser exposure time by lowering integration times. However, as the integration time is reduced, the signal-to-noise ratio of the Raman spectrum is also reduced. The operator must determine a balance between biological material damage and signal strength. The choice of the laser power, together with the magnification of the objective lens, governs the power applied per unit volume of the analyte. A larger spot size allows the use of larger powers. Generally, at magnifications of 40× or higher it is better to keep the laser power under 1 mW for large exposure times. This is a case where microfluidics are able to benefit Raman microscopy, as flowing fluids tend to dissipate heat energy and remove damaged analytes from the focal region, thereby allowing higher laser powers to be used. However, the eventual effect depends on the thermal conductivity of the medium and the parameters of the flow.<sup>59</sup>

### 2.3.6 Memory effect

Aside from the many benefits of Raman-microfluidic integration, there are still a many challenges. One such challenge is the possible “memory effect”. This is due to some particles and analytes sticking to the surface of the microchannels, causing permanent Raman background signals. Many strategies can be devised to eliminate this problem. For example, disposable chips can be used to avoid such memory effects. However, if reusable chips are desired then the walls should be carefully cleaned after each usage or they should be protected during the process to avoid any target analyte interaction with them. For instance, a segmented flow system can be implemented, in which a thin layer of oil is used to protect the microchannel walls from contamination.<sup>27,60-62</sup> There are also many other methods that can be applied to alter the hydrophobicity of the walls and substrate, reducing the occurrence of memory effect issues.<sup>63</sup>

### 2.3.7 Portability

One of the challenges presented to the Raman-microfluidic community is the issue of portability. Microfluidic systems are highly portable, being small sized and relatively robust. However

the dimensions of Raman microscopy units can be much larger, and particularly in the case of coherent Raman scattering, the alignment of the sample relative to the instrumentation can be critical placing stringent constraints on the optical interface to the microfluidic chip.

Low cost hand-held Raman spectrometers have spectral resolutions not exceeding 20 cm<sup>-1</sup> Raman shifts, while the resolution of laboratory spectrometers with optimised diffraction gratings, optical path lengths and cooled charged-coupled detectors can be as small as 0.1 cm<sup>-1</sup>. Similar concerns also apply to spatial resolution, while cost is a major determining factor for the sensitivity of the detector. Lower sensitivity spectrometers require higher laser power, which in turn limits the types of samples that can be analysed, particularly organic materials that can be damaged at high powers.

Efforts to reduce the size and complexity of the supporting optical equipment are underway; covering ideas such as creating on-chip laser sources<sup>64,65</sup> and replacing the confocal lens with other devices such as waveguides<sup>66</sup> and fibres.<sup>67,68</sup> Recently designed “Kinoform” microlenses for focussing into microfluidic channels can potentially be used in Raman systems.<sup>69</sup> Despite these advances, the greatest difficulty in achieving portability is reducing the size of the optical spectrometer while maintaining acceptable resolutions.

## 2.4 Materials

The type of material is an important consideration for systems that integrate Raman microscopy and microfluidics. From a microfluidic perspective, it is important to know what materials the device is fabricated from, and what target materials are to be interrogated. This is mainly to assure the least interferences from unwanted materials and the largest signals from the target analytes to be obtained by the Raman system. This section aims to highlight the various types of materials, and what considerations must be made for Raman-microfluidic devices.

### 2.4.1 Metals

Pure metals in bulk form do not produce any Raman signature; this is due to the presence of free electrons in the metal structure, which block the incident light from reaching the material bonds. This property makes metals reflective and gives them their high electrical conductivity.<sup>70</sup> However, very thin films of pure metals have been shown to produce Raman signatures, as the conductivity of nanometre thin films is low enough to allow photons to reach the metallic lattice bonds.<sup>71</sup> Nano-colloids and other roughened nanostructures are also capable of producing surface-enhanced Raman signatures, as discussed in the “Variations of Raman spectroscopy” section. The used of metal films or colloids to enhance Raman scattering is particularly applicable to microfluidic devices.

### 2.4.2 Non-metals

Raman microscopy is capable of providing a good representation of inorganic, non-metallic materials; providing information regarding their chemical bonds, lattice and crystal arrangements. This capability is particularly useful for identifying different morphologies of materials, inorganic polymorphs as well as differentiation of amorphous and crystalline material phases.<sup>70</sup> Metallic oxides have unique Raman signatures as seen in examples such as TiO<sub>2</sub>,<sup>71</sup> WO<sub>3</sub>,<sup>72</sup> and MoO<sub>3</sub>.<sup>73-75</sup> Additionally, Raman scattering can provide unique information regarding the

Cite this: DOI: 10.1039/C3CS35515B

www.rsc.org/csr

CRITICAL REVIEW

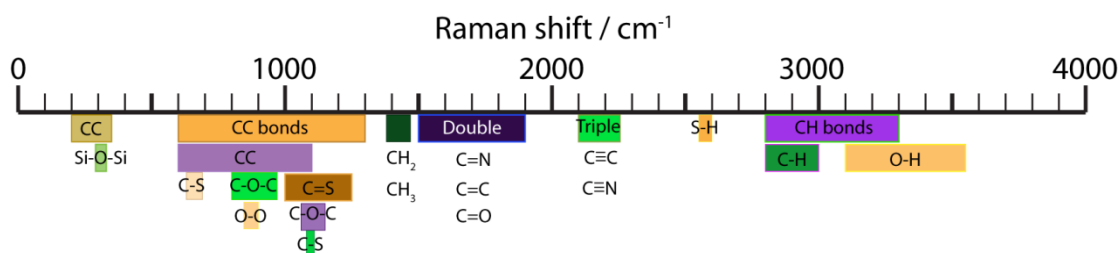


Fig. 3 Raman peak shift ranges for organic bonds

structure of materials like graphene, where it is possible to identify the number of layers and degree of oxidation in its structure.<sup>76</sup> Metal oxides can be used with microfluidic system as either trace analysis detection,<sup>29,62</sup> interrogating the purity of samples,<sup>77</sup> or the metal oxide particles can be used to track non-active Raman elements inside a microfluidic device.<sup>78</sup> Non-metals such as glass, silicon and quartz are frequently incorporated in the structure of microfluidics, which will be discussed in the “Microfluidic configuration and requirements” section.

### 2.4.3 Organic materials

Organic materials are important in the context of constituents that form the microfluidics devices and the target material to be interrogated using the microfluidic-Raman system. Changes in the character or quantity of particular organic bonds can be readily assessed by the location, strength and width of the Raman peak shifts. As mentioned earlier, the Raman signatures provide detailed information regarding rotational and vibrational properties of organic bonds. These Raman signatures can be well correlated with Fourier transform infrared (FTIR) signatures. FTIR spectroscopy is usually used together with Raman microscopy for the analysis of organic materials. Although FTIR and Raman spectra are similar, their signatures are not always identical. Polar organic molecular bonds, such as C-O, N-O and O-H, produce relatively weak Raman signatures but strong FTIR signatures. Conversely, neutral bonds such as C-C, C-H and C=C, are less easy to identify with FTIR, however they produce strong Raman peaks (Fig. 3). In the design of the microfluidics, care should be taken to avoid the interferences from the organic material components of the microfluidic structure, which will be fully discussed in the “Microfluidic configuration and requirements” section.

Raman-microfluidic systems are great tools for providing high resolution and sensitive information regarding changes in cell metabolites and proteins, demonstrating distinct differences between cells at various stages of cancerous growth<sup>79</sup> and can distinguish between healthy tissue, cancerous tissue and even pre-cancerous tissue.<sup>80,81</sup> Raman microscopy is also useful in measuring the type of polymeric materials in microfluidics, and their degree of polymerization. However, organic materials can be damaged by high energy, low wavelength excitation sources as they expose the organic bonds to high energy photons. To

accommodate this issue, Raman microscopy for organic, biological and medical specimens typically uses near infrared (NIR) lasers, such as 785 nm or 1064 nm, to reduce the photon energy. This, however, reduces the intensity of the Raman scattering process and necessitates highly sensitive Raman spectrometers and longer integration times. Regardless, NIR Raman microscopy has successfully been implemented in microfluidics to classify epithelial pre-cancers and cancers.<sup>82,83</sup>

The ability of Raman microscopy to interrogate small detection volumes can be used for the targeted analysis of larger organic objects such as cells and tissues. Raman microscopy can be used for the identification of individual cells, which have been sorted and filtered using microfluidic components. The system can produce even more targeted information, with Raman signatures being taken from various parts of a larger object, for example, targeting a cell where the Raman spectra of the nucleus, cell wall, cell membrane and cytoplasm can be acquired.<sup>2</sup> This powerful option allows the detailed analysis of a cell's health, or the ability to monitor the absorption of certain chemical drugs.<sup>84</sup> Another example has shown that different locations on a yeast cell produce markedly different SERS spectra.<sup>85,86</sup> Optical power density is again an important consideration when dealing with biological materials. Exposure to high optical powers has very detrimental effects on a cell, not only thermally, but the high energy can irreversibly damage and even kill a cell.<sup>57,87</sup> For microfluidic systems the risk of damage from high energy optical systems must also be considered, as high optical power can also affect the structure of the microfluidic device, causing undesirable fluorescence and background signals to be introduced.

### 2.4.4 Aqueous media and microfluidics

Aqueous media are the basis of microfluidics. Pure water produces weak Raman peaks at 1640 cm<sup>-1</sup> and at 3300 cm<sup>-1</sup> (Fig. 4) and can be readily used for suspending organic materials, particles and analytes.<sup>88-92</sup> Water is also the main medium used to store and culture living bio-materials. These benefits are what make Raman microscopy so powerful for microfluidics. The confocal ability of Raman microscopy allows targeting specific areas inside an aqueous suspension, with the ability to perform 3D Raman mapping. Furthermore, the intensity of the Raman peaks can be used to determine the local concentrations of suspended materials in addition to material identification as

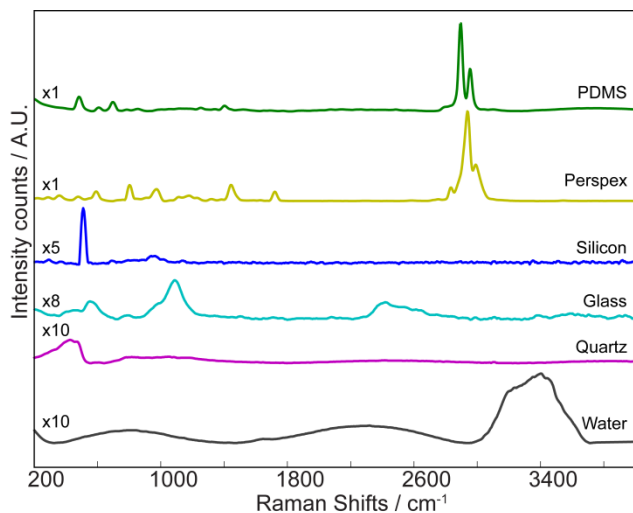


**Fig. 4** Normalised Raman spectra of possible microfluidic substrates such as PDMS, perspex, silicon, glass, quartz and water

described previously.

5 Some fluids have strong Raman signatures, which can be used for their identification and assessing their concentration in the microfluidics. Some of the examples of such measurements are presented in the “Applications” section. Examples of Raman studies of aqueous media include alcohols, which show a strong presence of CH and C=C bonds and produce Raman peaks at 1400–1900  $\text{cm}^{-1}$ . Additionally, Raman spectroscopy operates not only on transparent samples but also on many semi-opaque and opaque environments in microfluidics, for which many other optical systems fail.

### 15 3. Microfluidic configurations and requirements

Integration of microfluidic and Raman microscopy systems requires many engineering steps. There are a number of considerations for the integration of Raman microscopy with microfluidic systems, specifically relating to the design and fabrication of the microfluidic platforms. It is also important to highlight the potential benefits that microfluidic components such as mixers, filters and trappers can bring to integrated systems.

#### 3.1 Fabrication

Microfluidic systems are designed to deal with the behaviour, manipulation and precise control of fluids.<sup>93,94</sup> Microchannels are used to constrain the fluids to small scale areas, with some microchannels being less than 100 nm wide.<sup>95</sup> This small size allows for the accurate control of flow, making such channels suitable for the study of suspended materials and spatial mapping with high resolution. Microfluidics not only enable very precise flow control, but also has the potential for manipulation of materials suspended in the liquid media by utilising mixing and separating to optimise different chemical constituents.<sup>96,97</sup> Microfluidic systems can easily be interfaced with standard laboratory equipment such as syringe pumps, microscopes and electronic equipment to enhance the usefulness of their application.<sup>98</sup>

A further benefit of microfluidic devices is the ease of fabrication. “Soft lithography”, a phrase coined by Whitesides *et al.*,<sup>99</sup> is used to describe the processes for polydimethylsiloxane

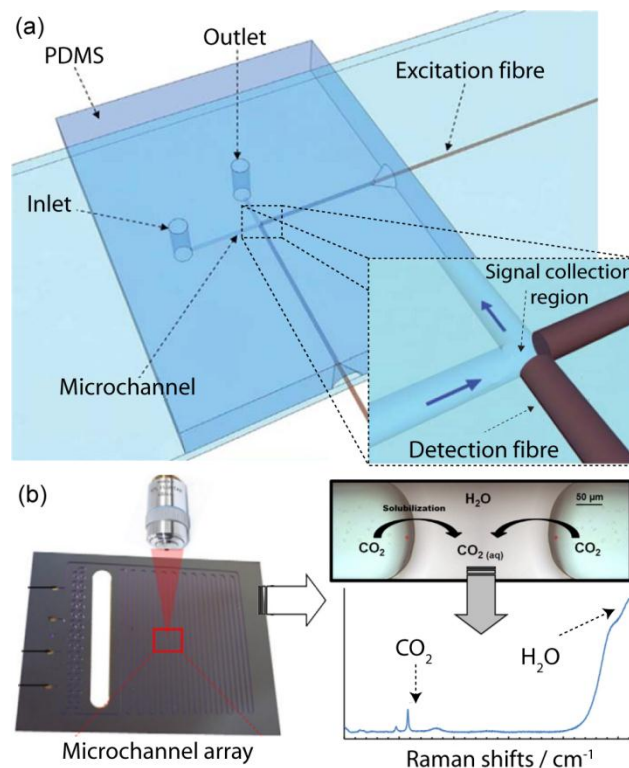


**Fig. 5** Raman system integration with microfluidic environments. (a) Integration of optical fibre detection into a microfluidic device for the purpose of *in situ* Raman detection. Reproduced from Ref. 66. (b) Confocal Raman microscopy demonstrating the detection of CO<sub>2</sub> solubility in water. Reproduced from Ref. 100 (Copyright (2012), with permission from Elsevier).

(PDMS) microfluidic device fabrication. Many other materials, such as glass, silicon and SU-8, can also be used for creating microfluidic devices, each with a focus on a different application.<sup>101</sup> As such, studies have been conducted to understand the properties of these materials, their biocompatibility and their effects on analysis performed in microfluidics.<sup>102</sup> Much research has been conducted into microfluidic substrate choice and fabrication methods, with detailed analysis of such methods available in the literature.<sup>10,101,103-107</sup>

Microfluidic devices based on rigid materials such as glass and silicon are often the basis of reusable systems and where severe chemical environments might be used in the microfluidics. However, the fabrication processes can be lengthy and require the use of high cost facilities and harsh chemicals. Conversely, PDMS is a relatively cheap material for the rapid fabrication of microfluidic devices. However, for PDMS based microchannels there is still a need for a rigid structural platform. This substrate can be made from anything with solid structural integrity, biocompatibility and preferably optical transparency. In fact, for Raman microscopy, a Raman transparent and low fluorescent material at the desired excitation wavelength is necessary.

Microfluidic devices can introduce significant Raman ‘background noise’ from the substrate and structures surrounding the microchannels. Such background noise is more noticeable if the channels are made of polymers with strong Raman signals (e.g. PDMS) and if the detection site is within close proximity to the polymer, or the imaging must be done through a polymer

membrane. This can be overcome by adding a Raman transparent window into the microdevice.<sup>40,108</sup> Raman signatures of various materials have been acquired using a 532 nm laser source and are depicted in Fig. 4. PDMS and Perspex have many characteristic Raman peaks throughout the entire spectral range, making them unsuitable for use in the path of the excitation laser. Silicon is usually used to ensure the correct alignment of Raman spectrometers, as it has a predictable and strong Raman peak at 520 cm<sup>-1</sup>. Glass has a very large and broad Raman peak near 1000 cm<sup>-1</sup> making it unsuitable as a microchannel substrate for detecting analytes with signatures around this range. Advantageously, quartz has relatively few Raman peaks, with only a broad peak at around 350 cm<sup>-1</sup>. As a result, quartz is an excellent material as the substrate of choice for Raman-microfluidics systems.

### 3.2 Optical transducers and environmental control

The measurement of parameters in microfluidics is performed using transducers, which are required to operate with high sensitivity on small volumes of fluids. Examples of potential parameters to monitor include flow rate,<sup>109,110</sup> viscosity,<sup>111</sup> heat transfer,<sup>59</sup> temperature,<sup>112</sup> electrical impedance,<sup>113,114</sup> permittivity,<sup>115</sup> refractive index<sup>116</sup> and other optical properties.<sup>117</sup>

Transducers can be integrated into microfluidic devices in a variety of ways: onto the surface of the substrates, on the walls of the microchannels or integrated within the microfluidic structures. They can be in direct contact with the fluids, or they can be fabricated so as to enable contactless detection. Some examples of non-optical, non-contact methods of detection that exist include capacitance sensors,<sup>113</sup> piezoelectric transducers<sup>118-120</sup> and magneto-electronic detection.<sup>121</sup> Transducers can be electrochemical, acoustic, thermal, electromagnetic and optical.

The emphasis of this review is the integration of Raman spectroscopy; however other transducers are in place to assist this purpose. A good example for integrated optical detection is shown in Fig. 5(a), in which an optical fibre is used for Raman spectroscopic detection of the analyte (in this case urea) in a microfluidic channel.<sup>66</sup> Similar fibre based Raman and SERS systems with direct fluid contact have been proposed by others.<sup>122</sup> This method requires the optical fibre probes to be in direct contact with the fluid, exposing the fibre to possible fouling and eventual damage. On the other hand, contactless optical detection in microfluidics can also be implemented, in which the laser is focused via an objective lens onto the area of interest for detection in microfluidics. Some recent examples include the evaluation of microfluidic mixing using confocal optical imaging to monitor the mixing of water and fluorescein dye<sup>123</sup> and the detection of gas using a PDMS microchannel design integrated with confocal fluorescence imaging.<sup>124</sup> Studies of CO<sub>2</sub> solubility in water (Fig. 5(b))<sup>100</sup> and metal oxide nanoparticle concentrations<sup>108</sup> are examples of Raman-microfluidic systems for online monitoring applications. A number of excellent review papers summarise the many optical transduction methods used in microfluidics.<sup>5,125,126</sup>

### 3.3 Considerations on flow, mixing, filtering and trapping

Careful control of the microfluidic environment is required to capitalise on the high sensitivity and selectivity of Raman microscopy systems. Regulation of the flow rate is critical, as

integration times for Raman spectroscopy are in the order of millisecond, seconds, and even minutes for some samples. The longer acquisition times require the targets to remain in the focal area for the duration of the integration. An alternative would be to implement microfluidic based traps to hold samples in the Raman target area for the duration of the acquisition time. These traps could be readily used for sorting purposes also, as Raman microscopy information regarding the target can be used to control the sorting process.<sup>117</sup> Furthermore, enhancement of the samples Raman signatures can be made using SERS, which would reduce the sample acquisition times. However, for many Raman-microfluidic systems, especially those based on SERS and for monitoring reactions (microreactors), it is necessary to ensure comprehensive filtering and mixing of the target materials, nanoparticles and analytes. This section will highlight the considerations on flow, mixing, filtering and trapping for Raman-microfluidic systems.

#### 3.3.1 Flow systems and mixers

One advantage of microfluidic systems is the ability to provide continuous flow, while still using small volumes of samples. The integration of microfluidic flow cells with Raman analysis is important as it allows for the analysis of small volumes by positioning the sample liquid into the Raman system detection area. Moreover, a higher reproducibility can be achieved in flow systems in comparison to static conditions due to the averaging effect over target material, and better heat dissipation of flow systems. Flow in microfluidics can be driven by pressure or vacuum using external pumps.<sup>127</sup> Other mechanisms also exist, such as capillary and electro-osmotic flows. The flow mechanisms in the microfluidic environment have been comprehensively reviewed.<sup>128-130</sup>

Mixing is an important aspect to be considered in Raman-microfluidics, as most microfluidic systems have low Reynolds numbers and therefore intermixing is diffusion limited.<sup>131</sup> Low Reynolds number systems are characterised by the absence of turbulence, and the dominance of a laminar flow within the system. Examples of laminar flow are seen in many microfluidic structures, especially in T-junctions (Fig. 6(a)), where the fluids are not immediately mixed after entering the junction and only intermix gradually through diffusion.<sup>132</sup> Raman beam rastering is one of the most efficient ways of assessing the degree of diffusive intermixing, which will be discussed further in the "Applications" section. Additionally, laminar flow systems can be manipulated and used for diverting streams of fluids, as shown in Fig. 6(b) - (e).<sup>133</sup>

As suggested in the introduction to this section, mixing is an essential part of many Raman-microfluidic systems especially microreactors and SERS based systems. Microfluidic mixers are implemented to enhance SERS signals, as mixing is vital for initiating chemical reactions and introducing particles or nanostructures that enhance Raman through SERS. If liquid mixing is desired, then special systems must be implemented in order to induce disturbances and enhance the mixing ability. Microfluidic mixers are often used for accelerating the reaction of chemical constituents. Mixers can also be used for the creation of precisely controlled nanoparticles, such as polymer beads<sup>134</sup> or metallic colloids.<sup>135</sup> The mixing between a silver or gold colloid and a target analyte must be as comprehensive as possible for

Cite this: DOI: 10.1039/C3CS35515B

www.rsc.org/csr

CRITICAL REVIEW

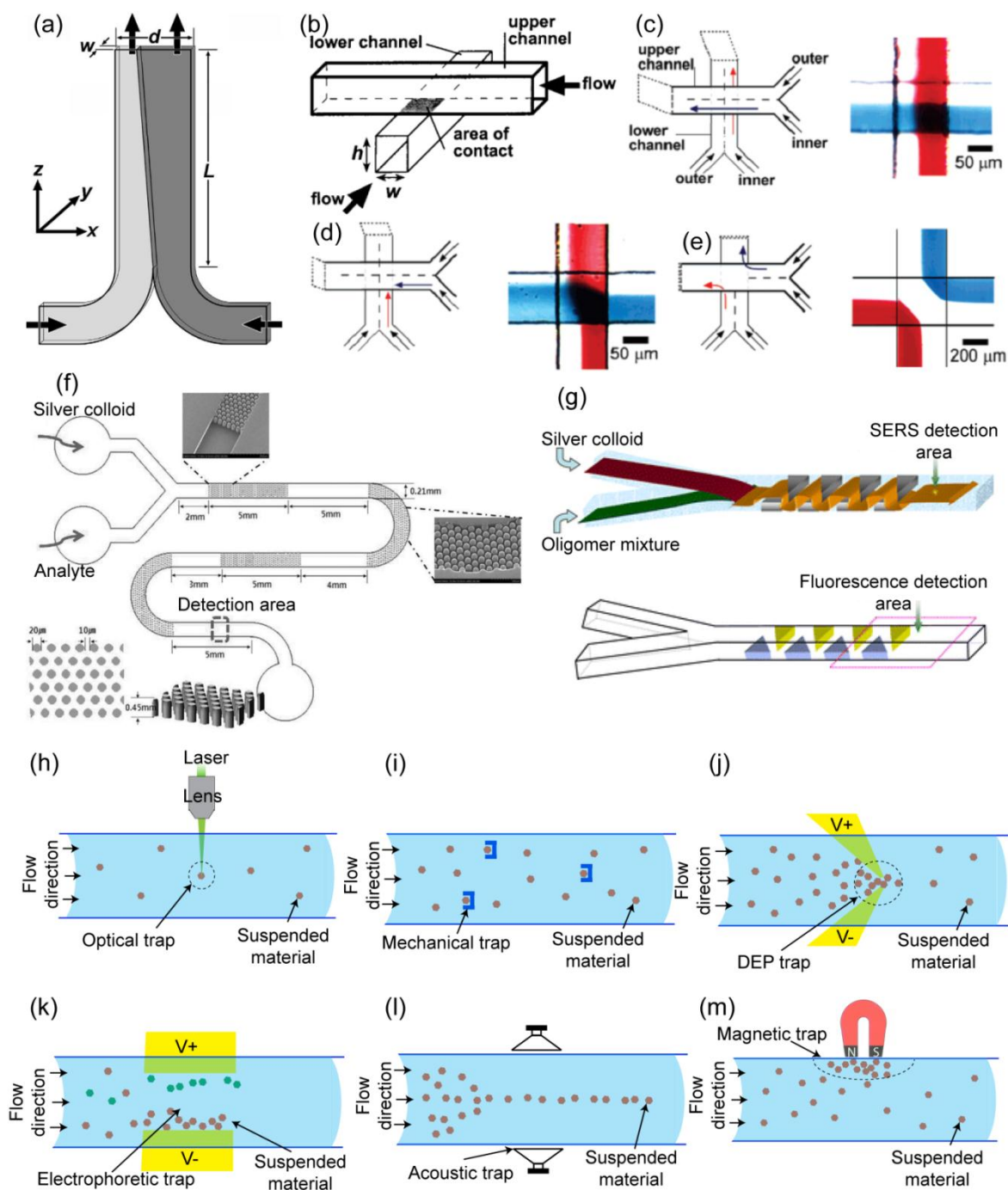


**Fig. 6** Microfluidic methods demonstrating flow principles, mixers and traps. (a) Conceptual rendition of the simplest form of the T-section system, where two fluid inputs enter through channels at the bottom and slowly diffuse over the length of the microchannel. Reprinted from Ref. 132 (Copyright 2001 with permission from Elsevier). (b) Schematic drawing of tangential microchannels, where the channels can exchange fluid through the shaded area of contact. Laminar flow experiments with the aspect ratio,  $A$ , of the contact areas as: (c)  $100 \times 160$ ,  $A=1.6$ ; (d)  $100 \times 44$ ,  $A=0.44$ ; (e)  $400 \times 25$ ,  $A=0.063$ . Adapted from Ref. 133 (Copyright (2001) American Chemical Society). (f) Schematic illustration of a pillar array PDMS based microfluidic channel for the SERS detection of hazardous materials. The dashed rectangle denotes the Raman measurement area. Reproduced from Ref. 136. (g) Schematics of alligator teeth-shaped micromixer. (h) Schematic examples of microfluidic traps using forces using: (h) optical (i) mechanical (j) dielectrophoretic (k) electrophoretic (l) acoustic and (m) magnetic forces

Cite this: DOI: 10.1039/C3CS35515B

www.rsc.org/csr

## CRITICAL REVIEW

obtaining high intensity SERS signals. Raman microscopy is capable of detecting many liquid and solid components from microfluidics, however it is also possible to monitor mixtures of those components. Even more relevant is the ability to use Raman microscopy for monitoring the mixing process itself, where Raman microscopy can provide information on desired and undesired chemicals produced during mixing (and possibly a reaction progress) as well as giving an indication of the quality of output chemicals from micromixers. However, from a microfluidic perspective, mixing only by diffusion is a time-consuming process, and relatively long microfluidic channel lengths are needed. A number of active or passive micromixers have been developed to address this problem.<sup>137</sup> Active mixers can achieve excellent mixing, but are comparatively difficult to integrate with other microfluidic components as they are relatively costly and generally require complex control units and external power sources (e.g. bubble-induced actuators, magnetic stirrers, or ultrasonic wave generators). Passive micromixers are not as efficient and rapid but offer the advantage of easy integration with other microfluidic components, low cost and no external power source.<sup>29,123</sup> Examples of passive mixers are demonstrated in Fig. 6. Micropillar microchannels for the mixing of silver colloids with chemicals such as dipicolinic acid have been demonstrated (Fig. 6(f)).<sup>136</sup> In a similar concept, alligator teeth-shaped PDMS channels have been used for effective mixing of silver colloid with DNA oligonucleotides (Fig. 6(g)).<sup>51</sup>

### 3.3.2 Traps, filters and sorters

Trapping, filtering and sorting of suspended materials can be implemented in a microfluidic environment. For Raman detection and screening applications it is important to analyse specific bonds within small and/or low concentration sample volumes. This requires relatively long acquisition times, therefore the target should be immobilised for investigation. This is especially important in the analysis of bio-cells in clinical experiments. Therefore, various trapping, sorting and filtering methods for delivery of bio-components and cells to the detection area of Raman systems and sorting of them with the use of microfluidic devices, are essential.<sup>138</sup> All of these functions can be performed through the application of some type of force. The separation of materials, especially biological materials, is essential for processes where purer samples are desired. The active separation forces that can be readily applied include optical, mechanical, electrokinetic, magnetic and acoustic (Fig. 6(h) – (m)).<sup>117</sup>

In microfluidics, optical beams are commonly used for trapping (also known as tweezing) suspended objects, allowing interrogation of these particles using optical methods such as fluorescence or Raman microscopy (Fig. 6(h)).<sup>139</sup> Optical trapping can be performed using the Raman excitation laser or a separate laser beam using single or multiple objectives or fibres. In a recent example, optical traps have been used for isolating bacterial cells in liquid media.<sup>56</sup> It is possible to then change the content of the fluid environment surrounding the cells by holding them in a trap while continuing to monitor their response. Further

to this approach, a waveguide optical trap was recently used on yeast cells.<sup>140</sup> The waveguide trap has the advantage of causing minimal damage to the cells due to the low optical power of the evanescent field. The use of optical traps is widespread for analysing cells in fluid environments, and many trap designs have been demonstrated.<sup>67,141-148</sup>

In microfluidics, mechanical traps require no external inputs beyond the fluid flow itself in order to operate, and can also allow for the controlled release of the trapped objects through manipulation of the flow. Mechanical traps use specifically designed barriers for holding objects in position, and are usually implemented for long term studies, including studies of cells (Fig. 6(i)). If an object in such a mechanical trap is to be interrogated using Raman microscopy, it has to be considered that the materials used in fabricating such traps can also interfere with the Raman signals. Examples of mechanical traps include those for holding single cells, where air bubbles are then used to eject the cells at the end of the measurement cycle.<sup>149</sup> Other examples use mechanical traps for the optical imaging of live cells in microfluidics, while allowing for the ability to modify the fluid environment without disturbing the imaging process.<sup>150</sup>

Electrokinetics is a broad term that covers many phenomena that occur in fluid environments, specifically involving the double-layer surrounding the suspended materials and the electrical properties of both the media and materials. The most studied concepts of these effects, implemented in microfluidics for separation and trapping, are dielectrophoresis (DEP) and electrophoresis.<sup>117,151-156</sup> DEP is defined as the force exerted on a suspended dielectric particle in the presence of a non-uniform electric field. The magnitude and direction of the force is related to the electric field intensity, particle radius, permittivity of the particle and suspending fluid, as well as the conductivity of both the particle and suspending fluid (Fig. 6(j)). DEP can be used for trapping and sorting almost any type of suspended materials ranging from nanoparticles and carbon nanotubes<sup>157</sup> to cells<sup>158</sup> and DNA.<sup>159</sup> DEP based cell traps have been used for quantifying the per-cell levels of lactic acid production<sup>160</sup> as well as the trapping of DNA with specific strand lengths.<sup>159,161</sup> Sorting systems based on DEP have been used for sorting cervical cells into healthy and tumorous types and can potentially be used as an early detection device for cervical cancer.<sup>162</sup> Other systems demonstrate the separation of bacteria and yeast cells based on their differing dielectric properties.<sup>157,158</sup> DEP has been integrated into Raman-microfluidics for the trapping and mapping of nanoparticles such as WO<sub>3</sub>.<sup>108</sup> It has also been used for controlling the dynamic spacing between silver nanoparticles for optimising the SERS signals of biomaterials.<sup>30</sup>

In microfluidics, electrophoresis can be used to move suspended particles under the influence of uniform electric fields. For particles with a surface electric charge, the electrophoresis process is affected by surface adsorbed species, and as a result the external electric field exerts a motive Coulomb force (Fig. 6(k)). An application of electrophoresis has been demonstrated for the

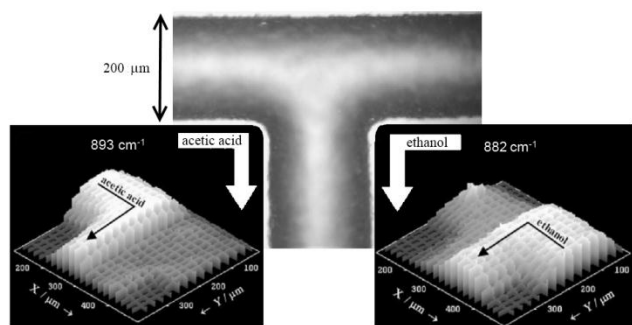


**Fig. 7** A T-junction microfluidic channel approx. 200  $\mu\text{m}$  wide for the purpose of mixing ethanol and acetic acid. Insert images show rasterised Raman images of acetic acid and ethanol using their respective Raman peaks. Adapted from Ref. 163 (Copyright 2003 Wiley-Liss, Inc)

separation and detection of chemicals in a hybrid SERS nanocomposite device.<sup>164</sup>

There are many more methods for trapping and sorting objects in microfluidics,<sup>165</sup> including acoustic<sup>166</sup> and magnetophoretic processes,<sup>167</sup> which are yet to be integrated with Raman systems. Schematic diagrams illustrating these processes are presented in (Fig. 6(k) – (m)). Thermal procedures can also be considered.<sup>168</sup> Interested readers are referred to comprehensive reports which dissect the various methods into two categories, active and passive, and proceed to analyse their resolution, throughput and efficiency.<sup>169</sup> It is also noteworthy to include a final example reported by Lutza *et al.*<sup>170</sup> who used Raman spectroscopy to image the eddy concentration distribution for various acoustic oscillations in microfluidics.

## 4. Applications

As discussed previously, both microfluidics and Raman spectroscopy are extremely useful methods in their own right. The integration of the two allows us to capitalise on all of the benefits available to microfluidics, such as low analyte volume, tight control of the microfluidic environment and portability. Additionally, Raman microscopy provides detailed analysis of the target materials in microfluidics, including information from suspended solids, liquid and dissolved gaseous samples and their environments.

### 4.1 Investigation of analytes

One of the most important features of Raman spectroscopy is that it provides information relevant to the quantity and types of chemical bonds in the sample. The Raman laser beam can be readily focused into a small volume of material within a microfluidic system and allows analysis of only that very small volume. Raman-microfluidic devices also show great promise for the detection of analytes in complex mixtures, as accurate measurements of different analytes can be simultaneously conducted.<sup>126</sup>

Many organic liquids can be efficiently detected with Raman microscopy as they have a strong Raman cross-section. There are many reported examples that have exploited this property. For instance, Fletcher *et al.*<sup>163</sup> studied a T-shape microfluidic device for the mixing of ethanol and acetic acid. Raman microscopic mapping was used for detecting the two analytes at various mixing stages. The results show a very well controlled laminar

flow in the system. Fig. 7 depicts the Raman beam rasterised image of the T-channel, demonstrating the accuracy of analyte detection in a microfluidic environment. This method uses two distinct Raman peaks for the detection of ethanol ( $882\text{ cm}^{-1}$ ) and acetic acid ( $893\text{ cm}^{-1}$ ), and can only be applied to those analytes which have non-overlapping Raman peaks. There are many more examples of such applications.<sup>132,171-173</sup>

Microfluidic micro-reactors are used for the careful control and study of reactions. Raman microscopy can be incorporated in such systems to investigate small volumes, determining the presence of analytes and catalysts during the entire reaction process. Raman microscopy offers high-information content, in-line detection within microfluidic based micro-reactors. A very good example is found in the work of Leung *et al.* who used a continuous flow micro-reactor with in-line confocal Raman microscopy to measure the concentration of output constituents.<sup>174</sup> In their work, the catalytic oxidation of isopropyl alcohol into acetone was monitored in real-time. They were able to use the microfluidic environment to vary the input chemicals and control the product conversion to precise levels.

Detection of specific analytes in a liquid is something which is generally of interest for sensing, monitoring low concentrations of precious materials, and many other process control applications. When dealing with low concentration analytes it is important to have a good understanding of the target analyte and to assure that the parameters of the incorporated Raman system have been well tuned for the detection of those targets. For instance, Raman systems which use NIR excitation can be efficiently used for detecting, and accurately measuring the concentration of organic samples such as glucose, lactic acid and creatinine.<sup>126</sup>

Detecting low concentration analytes can be difficult using conventional Raman systems; however using SERS, SERRS, and TERS, with either fixed nanostructures or colloidal suspensions, it is possible to increase the apparent Raman cross-section of the target analyte. For these systems, pre-processors, such as mixers (see section “Considerations on flow, mixing, filtering and trapping”), are required to encourage the efficient bonding of target analytes onto the nanostructures that are used for enhancing the signals. Such systems have been used for sensing concentration levels in the part-per-million or even -billion levels of analytes such as cyanide, dipicolinic acid and malachite green (Fig. 8(a) – (b)).<sup>29,136</sup> There are many good review papers covering relevant topics in this field.<sup>21,23,175</sup>

Further enhancements of Raman signals can be achieved by controlling the spacing between the SERS colloid at the detection area. It has been shown that colloid spacings in the range of 1 – 10 nm produce significant enhancement over randomly positioned colloid.<sup>176</sup> This control can be either static or dynamic in nature. Static methods use organic and/or inorganic spacers that chemically attach onto the surface of colloids, which can be used for obtaining desired gaps between the particles.<sup>177,178</sup> The main drawback of such static systems is the lack of real-time tuning ability and the interfering Raman signatures seen from the spacers. Achieving dynamic spacing, without colloid aggregation, can be more challenging. One method for obtaining the optimum spacing has been demonstrated in our own laboratory,<sup>30</sup> where dielectrophoretic forces were used to control the spacing of

Cite this: DOI: 10.1039/C3CS35515B

www.rsc.org/csr

CRITICAL REVIEW

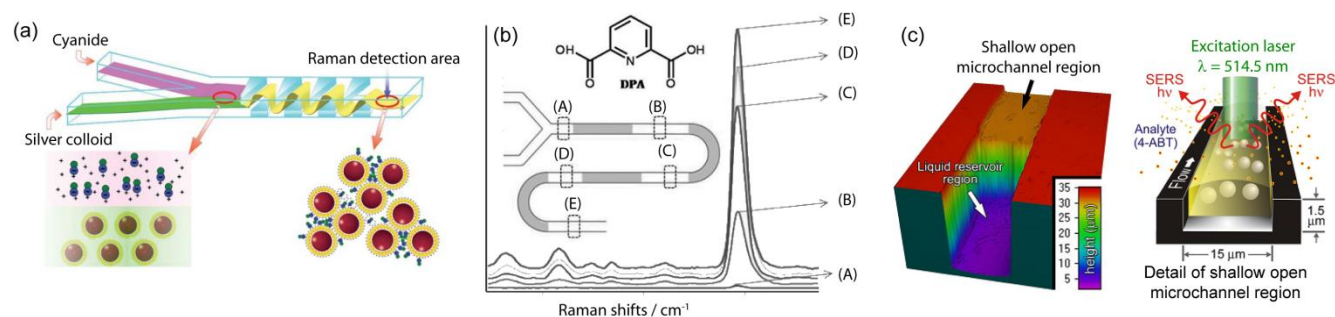


**Fig. 8** Raman-microfluidic device applications for detecting suspended analytes using SERS colloids. (a) Detecting of cyanide using a microfluidic mixer. Reproduced from Ref. 29. (b) Detection of dipicolinic acid using a micropillar mixer. Reproduced from Ref. 136. (c) Detection of 4-ABT using an open microchannel design. Reproduced from Ref. 25 (Copyright 2007 National Academy of Sciences, USA)

suspended silver colloid to detect low concentrations of dipicolinic acid.

The application of fixed nanostructures for the SERS enhancement of analytes in a microfluidic channel is also presented for the detection of many organic samples such as components of blood.<sup>179</sup> One of the challenges associated with these methods is ensuring enough analyte makes contact with the nanostructures within the microfluidic flow. Physical forces such as electrophoretic force can be used for bringing the target materials into the enhancement range of the nanostructures.

The use of similar techniques to detect airborne analytes presents a challenge, as these analytes must first be captured either by absorption onto solid substrates or suspended in water, after which Raman analysis can occur. In order to accommodate this, open channel microfluidics, where one side of the channel is exposed to the air environment, have been integrated with colloidal SERS (Fig. 8 (c)).<sup>25</sup>

#### 4.2 Materials science – nano/micro particles

The ability to identify and measure suspended materials is very useful with applications in assessing water contaminants and micro-reactor outputs, determining the concentration of mixtures and identifying unknown suspended materials. Raman-microfluidics can be employed for determining the quality of soil ingredients (after required pre-processing), chemical interactions, catalyst activities and corrosion effects.

Traditional methods of detection involve long preparation procedures, such as drying samples and/or centrifuging liquid samples to obtain more concentrated solutions. These procedures can be accelerated in microfluidic devices, after which Raman microscopy is capable of identifying many materials, delivering their chemical ‘fingerprint’.<sup>180,181</sup> A good example is demonstrated in the work of Chan *et al.*<sup>182</sup> where CARS detection of suspended sub-micron sized polystyrene beads was shown. This concept was then expanded for the trapping of unilamellar vesicles, where the Raman analysis indicated peaks present at 1440  $\text{cm}^{-1}$  due to the  $\text{CH}_2$  component in the lipids structure of the vesicles.

Many nanoparticles are synthesised and kept in colloidal forms, which are suitable for microfluidic processing. Raman microscopy can provide invaluable non-invasive information about such colloidal systems: the type of suspended nanoparticles can be identified, the colloid concentration can be determined using the intensity of Raman peaks and even the size of nanoparticles can be measured from the Raman peak shifts and their widths.<sup>183</sup> Raman microscopy can be efficiently employed for nanoparticles that generate surface plasmon resonances, such as gold and silver colloids, and can be used to determine their size during synthesis.<sup>184</sup> Raman-microfluidic systems are well-suited to analyse the interaction of chemicals and organic analytes on plasmonic nanoparticles.<sup>185</sup> Additionally, Raman microscopy can be used to determine other nanoparticles such as carbon based particles (carbon nanotubes, carbon black and graphene), metal oxides and chalcogenides using their strong Raman peaks.<sup>72,108,183,186</sup> The concentration of nanoparticles at different areas of the microfluidics can be mapped and their relation to the dynamic forces of the flow can be obtained.<sup>108</sup>

One difficulty with handling suspended materials in microfluidic environments is the ‘memory effect’. This effect is due to the attachment of materials to the inside surfaces of the microchannels, as discussed in the “Considerations for Raman microscopy in microfluidics” section. This memory effect can introduce unwanted Raman signals, giving false readings of concentration, and requiring the regular replacement of microdevices. In an effort to minimise these issues an oil/water interface is created on the inside surface of the microchannel to minimise the chance of material attachment. Additionally, the flow system is arranged to form micro-bubbles, or nanodroplets, of liquid in order to minimise the time the microchannel surface is exposed to potential fouling materials.<sup>27,60</sup>

In order to improve the magnitude of the acquired Raman signals, it is common to increase the concentration of the suspended material prior to analysis. Microfluidics provides the perfect platform for this step, as pre-concentration can be conducted on chip. Many different types of forces can be used for this purpose, such as ultrasonic standing waves<sup>187</sup> or

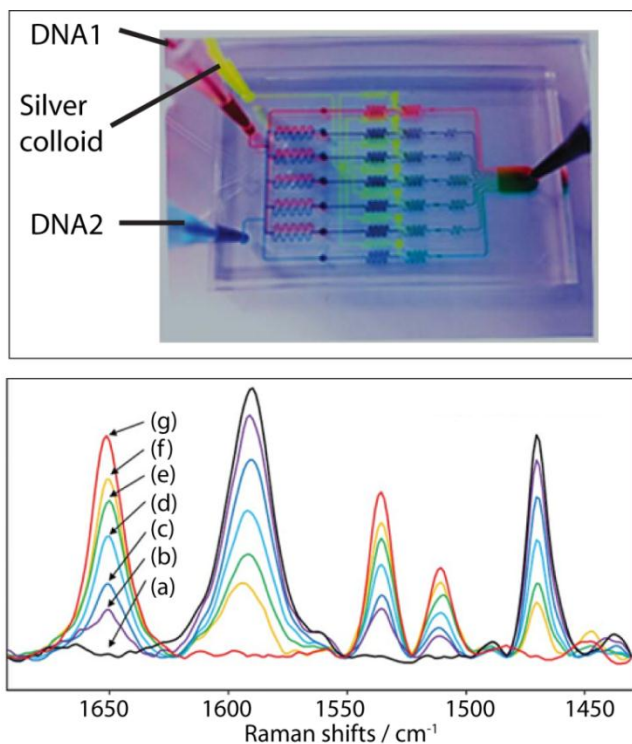


**Fig. 9** Raman-microfluidic devices for the mixing and detection of two breast cancer-related DNA types (DNA1: 5'-CTG TTT GCT TTT ATT-3'; DNA2: 5'-GCT GTT TAT TTA TTA-3'). Raman spectra of mixtures with ratios of DNA1 to DNA2: (a) 0:1 (b) 1:3 (c) 1:2 (d) 1:1 (e) 2:1 (f) 3:1 (g) 1:0. Reproduced from Ref. 188

dielectrophoresis.<sup>108</sup>

### 4.3 Analysing biological samples

Raman-microfluidic devices are ideal for analysing biological species, as they provide distinct 'fingerprints' for each of the samples and as such, have found many applications in biology and biomedicine. They are attractive devices for non-invasive biological studies as live samples can be analysed, they have high sensitivity to even molecular scale interactions and hence only very small sample volumes are required. This section addresses biological applications of Raman-microfluidic devices and highlights their uses in specific studies.

#### 4.3.1 Proteins

Proteins play important roles in many biological functions such as cell signalling, immune responses, cell structuring, cell adhesion and cell life-cycles. They are sensitive biological constituents requiring non-invasive and non-destructive measurement methods. Proteins are made up of chains of amino acids, which produce strong Raman signatures, specific to the type of amino acids. As a result, they can be differentiated with a good accuracy using Raman microscopy.

Proteins such as enzymes and antibodies, as well as carriers and membrane proteins, have been studied extensively in microfluidics.<sup>12,58,189,190</sup> Raman-microfluidic devices can be efficiently utilised in the study of the behaviour of proteins, their functionalities and their responses under various stimuli. Microfluidics can also be used for purification of proteins from other components of a cell and this entire process can be continuously monitored using Raman microscopy.<sup>191</sup> Enzymes and antibodies can be incorporated into microfluidics to establish

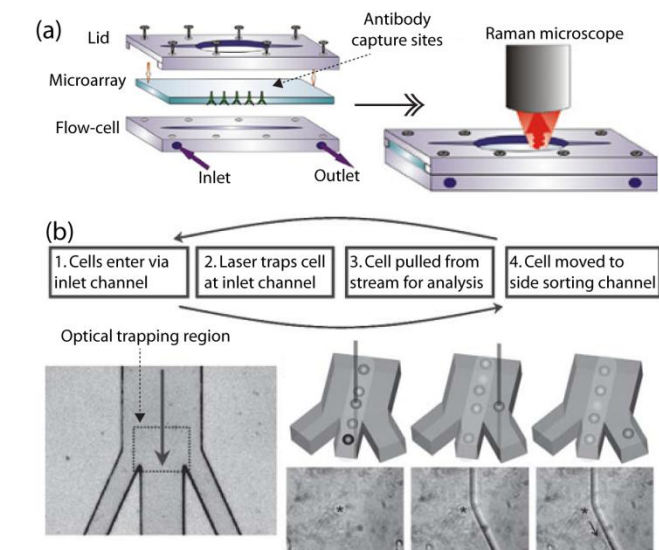


**Fig. 10** Applications of Raman-microfluidic systems for cell detection and sorting. (a) Schematic of a Raman-microfluidic device fitted with antibody capture sites. Cells are captured at these sites and are interrogated by Raman microscopy. Image not to scale.

Reproduced from Ref. 28 (with kind permission from Springer Science and Business Media). (b) Operating procedure and associated images for a Raman-microfluidic cell sorter using optical trapping and manipulation. Reproduced from Ref. 138

highly sensitive label-free and molecule-specific biosensors based on Raman microscopy.<sup>192,193</sup> Additionally, SERS, SERRS and TERS can be used for enhancing the detection of suspended proteins. An example by Yang et al involves the SERS detection of cytochrome *c* and lysozyme proteins from a suspension at various concentration levels.<sup>194</sup> Additionally, the SERS detection of BSA has been demonstrated using gold colloid, with detection limits as low as 100 pM.<sup>195</sup>

#### 4.3.2 Deoxyribonucleic acid (DNA) and ribonucleic acid (RNA)

DNA and RNA are the storage media for genetic information and are constructed from either ribose or deoxyribose sugars. The importance of nucleic acids is clear, and their identification and characterization is paramount for many research fields. DNA samples are employed in many applications including the recognition of genetic abnormalities and also used heavily for forensic identification. Other uses for DNA include genetic engineering, bioinformatics, disease identification and biosensing.<sup>196-200</sup> DNA produces Raman spectroscopic signatures and can be readily dispersed in aqueous media, making Raman microscopy well suited for detection in microfluidic systems that process DNA. The Raman detection of DNA is widespread through the use of SERS, as SERS provides the ability to coat colloids in DNA friendly substances.<sup>201,202</sup> The use of a microfluidic SERS mixer to detect single DNA oligonucleotides has been shown to accurately determine their concentrations.<sup>51</sup> The simultaneous detection of multiple DNA oligonucleotides using SERS has also been demonstrated, where a multi-gradient microfluidic channel was used for controlling the microfluidic environment. Labelling the DNA oligonucleotides can also assist in differentiating between the Raman signals (Fig. 9).<sup>188</sup>

For DNA monitoring in microfluidics, many issues should be taken into consideration. Polymerase chain reaction systems can

be integrated into the Raman-microfluidic device, providing enough DNA strands for the detection. The application of linkers, dyes and surface seeking groups are important factors as they allow for the efficient adhesion and immobilisation of the DNA strands for monitoring processes.<sup>37,38</sup> Pre-processing procedures such as mixing and filtering are also important in DNA Raman-microfluidics. As an alternative to colloid mixing, there are reported implementations that use solid microchannel features to achieve mixing and Raman enhancement.<sup>203,204</sup>

#### 4.3.3 Cells

The structure of a cell is complex, with many biological constituents in its make-up, such as proteins, DNA, amino acids and various other components. Raman microscopy is well suited to the simultaneous detection and selective analysis of the components of such complex mixtures. Additionally, cells are more active in liquid environments, where nutrients can be absorbed from the liquid, and communication chemicals released.<sup>205,206</sup> Microfluidic systems are ideal for sustaining cells in an aqueous environment where constant control of the chemical makeup and other environmental factors is possible.<sup>205,206</sup> Such control is especially important for extended studies where cells are cultured through their entire life-cycle. Furthermore, Raman microscopy can be used to monitor the chemical signatures of each stage of this life cycle and hence allows for the classification of cells into lifecycle states, including viable, necrotic and apoptotic.<sup>207-209</sup>

Raman-microfluidic systems are capable of identifying and studying contaminating cells, including bacteria, for situations such as water quality control and studying the effects of antibiotics on particular strains. A practical example of how Raman-microfluidic devices are used in such applications is demonstrated by Knauer *et al.*<sup>28</sup> A water quality monitor was developed in order to ensure that no *E. coli* cells were present per 100 ml of water, and was designed to have internal antibody capture sites for *E. coli*. (Fig. 10(a)) The system operation required a specific volume of water to pass through a microfluidic channel, fitted with *E. coli* trapping sites, after which silver colloid was introduced to coat any trapped *E. coli* cells. Using the prominent 565  $\text{cm}^{-1}$  Raman peak, the system was capable of detecting the presence of any *E. coli* cells, even down to the single cell level.

It is possible to take advantage of the high confocality offered by Raman microscopic systems for the analysis of individual components of cells, avoiding the need to destroy the cell. As an example, Raman analysis has been performed on suspended *Bacillus anthracis* spores to determine the amount of calcium dipicolinate contained inside the spores.<sup>210</sup> It is also possible to classify tumour cells depending on their internal chemicals, demonstrating how Raman-microfluidic devices can be used to identify specific types of tumour cells from a larger sample of unknown cells.<sup>67</sup>

Microfluidic systems can be implemented to filter and sort cells, with the ability to create highly pure cell samples. Raman microscopy is able to detect differences and defects in cells, and when coupled with suitable microfluidics, can be used as the sensor component of a cell sorting system. An optical trap has been used for such sorting, where lymphocytes were identified and sorted. Lymphocytes are vital to the human immune system and there are many variants with a range of specific functions.<sup>138</sup>

The cells are trapped at a Raman detection site where they are then categorised and positioned inside special holding areas, creating pure sample batches of the lymphocyte types (Fig. 10(b)). Microfluidic traps provide Raman-microfluidic systems with the capacity to study cells that are exposed to changing environmental conditions, with systems being used for studying the effects of medical drugs on cells. To this end, a Raman-microfluidic system to study the behaviour of yeast cells under various environmental conditions has been demonstrated.<sup>211</sup>

Temporal studies of cells are possible with Raman-microfluidic systems. As an example, Chinese hamster ovary (CHO) cells have been studied using a Y-shaped microfluidic channel used to mix cells with SERS colloid.<sup>212</sup> The cells were monitored over time using Raman microscopy, and it was found that Amide I levels reduced over time. Furthermore, spatial experiments were also conducted on the CHO cells, creating an x–y Raman map, together with a z–axis profile showed that there was a strong indication of C–H deformation peaks from proteins near the centre of the nucleus.

#### 4.3.4 Tissue

Raman-microfluidics has found applications in tissue engineering, where the benefits of such systems include the continuous flow of nutrients and vital gases like oxygen, as well as the constant withdrawal of waste products.<sup>213,214</sup> Additionally, microfluidics provides the perfect platform for studying fundamental biological phenomena, including exposing tissue to environmental variations at critical growth stages to monitor their effects.<sup>215</sup> The applications of this technology are particularly important for the study of drugs, where tests can be implemented safely on live human tissue samples in a highly controlled environment while allowing for accurate measurements. This could drastically reduce the failure rate of potential drugs involved in human clinical trials.<sup>216</sup> Some examples extend this concept as far as ‘organ-on-a-chip’ microsystems, which allow for *in vitro* organ-level studies, as opposed to cell-based systems.<sup>217</sup> Raman microscopy can be applied to these ‘organ-on-a-chip’ systems for in-line detection and monitoring of samples, providing accurate measurements of chemical constituents. Raman microscopy allows for non-invasive and non-contact detection in the LOC environment, providing contamination-free and well controlled results. With the use of SORS or transmission Raman it is possible to analyse 3D tissue samples, with penetration below the surface of the tissue samples, providing valuable feedback on the internal process of tissue samples.<sup>3,218-223</sup>

#### 4.3.5 Other organic samples

In addition to the aforementioned organic samples, Raman-microfluidic systems are capable of studying many other biological candidates, including DNA-cell, DNA-protein, virus, toxins and cell-protein complexes,<sup>224</sup> and their compositions with inorganic chemicals.<sup>200</sup>

Raman microfluidic systems are also excellent tools for investigating zygotes and embryos. The monitoring of zygotes and embryos in microfluidic environments that simulate their host are particularly important for the investigation of genetic deformations, abnormalities and related issues and provide invaluable information about the process of their growth. Raman microscopy has already been used to identify and study yeast

Cite this: DOI: 10.1039/C3CS35515B

www.rsc.org/csr

CRITICAL REVIEW

**Table 1** Comparison of Raman spectral analysis techniques

Technique	Description	Qualitative	Quantitative	Examples
Hierarchical cluster analysis (HCA)	Order Raman spectra into hierarchy of commonalities	YES	NO	Bacteria strain <sup>225</sup> respiratory syncytial virus strain <sup>226</sup> Bacteria on milk <sup>227</sup> Bacteria in food <sup>228</sup> Counterfeit drugs <sup>229</sup> Human blood <sup>230</sup>
Principal component analysis (PCA)	Reduce Raman spectra down to several principal components, determining the score values for each spectrum	YES	NO	Tetracycline antibiotics <sup>231</sup> Suppositories <sup>232</sup> Preeclampsia <sup>233</sup> Medicine counterfeits <sup>234</sup> Saliva from lung cancer patents <sup>235</sup> Laryngeal cancer diagnosis <sup>236</sup>
Partial least squares (PLS)	Multivariate regression technique where a set of known (expected) chemicals is compared against a complex spectrum in order to extract a linear relationship between the known concentration of a particular component and the intensity of Raman spectral information	NO	YES	Pharmaceutical tablets <sup>237</sup> Prednisone in tablets <sup>238</sup> Tetracycline antibiotics <sup>231</sup> Illicit street drugs <sup>239</sup> Suppositories <sup>232</sup> Human blood plasma <sup>240</sup>
Principal component regression (PCR)	Linear regression is used on the principal components of the Raman spectral data to obtain the quantity of the Raman principal components within a Raman spectrum (similar to PLS, without the known spectra)	NO	YES	Polyurethane <sup>241</sup> Gestational hypertension <sup>233</sup> Identification of medicine counterfeits <sup>234</sup> Laryngeal cancer diagnosis <sup>236</sup> Saliva from lung cancer patents <sup>235</sup>
Deconvolution	Breakdown of complex Raman spectra into known bond peaks in order to identify and quantify its components	YES	NO	Human skin samples <sup>242</sup> Cancer cells <sup>243</sup> Carbon nanotubes <sup>244</sup>
Wavenumber correlation	Comparing a known Raman spectrum to the unknown and determining its correlation	YES	NO	Tungsten trioxide <sup>108</sup> Graphites <sup>245</sup> Poly(L-lysine) <sup>246</sup>
Linear regression	The concentration of the sample is measured using the intensity and/or widths of Raman peaks, where a linear relationship between the known concentration values and the Raman spectral data is made	NO	YES	Dipicolinic acid <sup>136,247</sup> Promethazine <sup>60</sup> Glucose <sup>248,249</sup>

zygote cells in an effort to apply such Raman mapping for the label free study of cell proliferation.<sup>250,251</sup>

*In vitro* fertilisation (IVF) treatments currently rely on visual inspection of the morphology of an embryo in order to determine its viability as an IVF candidate. Research currently suggests that Raman microscopy can assist in the identification of ideal candidates, in combination with morphology characteristics,<sup>252,253</sup> with the potential to increase IVF success rates.<sup>252,253</sup> Furthermore, microfluidic environments can be used to enhance the monitoring and handling of embryonic cells, as microfluidics would allow for high throughput approaches.<sup>254-256</sup> The microfluidic environment can even be used for the fertilisation of embryos, allowing the initial stages to be carefully monitored before transferring the embryo to the host.<sup>254,255,257</sup>

#### 4.4 Pharmaceuticals

Raman microscopy can be used for investigating the effectiveness of developed drugs in the controlled microfluidic environment.

Different scenarios can be 'simulated' and tested using Raman-microfluidic systems, using low cost processes and small volume samples, before the pharmaceuticals are tested on animals and human. Multi-component pharmaceuticals can also be tested and the results categorised using multivariate data analysis procedures.<sup>258</sup>

Microfluidic micro-reactors can be used for pharmaceutical production and testing, and every stage of the process can be carefully controlled. Raman microscopy can be used to give real-time feedback on the chemical reactions in such systems.<sup>259</sup> For example, Raman microscopy can support the screening of polymorphic structures, and support the chemical development

Cite this: DOI: 10.1039/C3CS35515B

www.rsc.org/csr

CRITICAL REVIEW

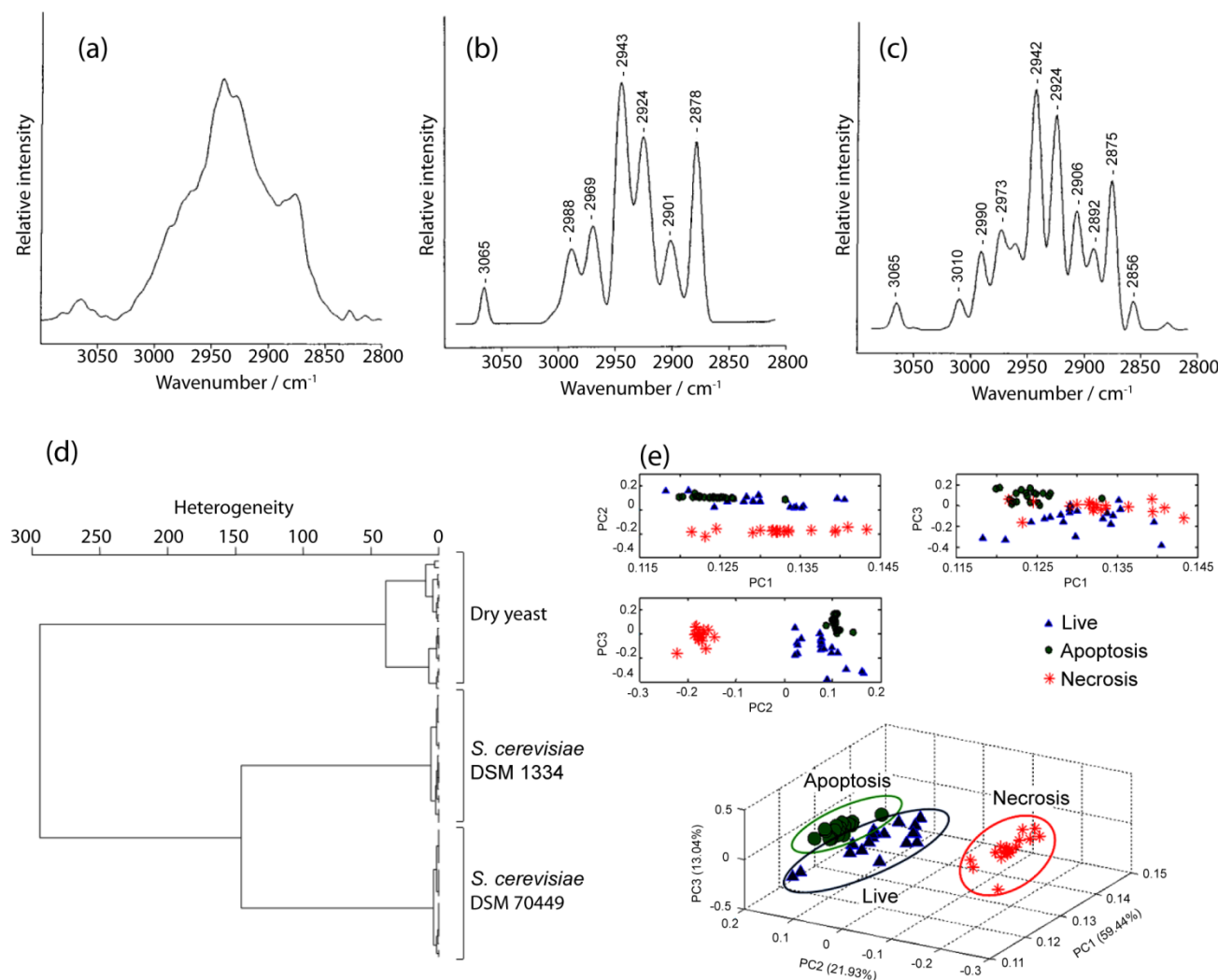


**Fig. 11** Examples of qualitative multivariable evaluation of Raman microscopic data. (a) Raman spectrum of  $\beta$ -lactoglobulin (b) deconvoluted spectrum using Lorentzian peak shape and (c) deconvoluted spectrum using Gaussian peak shape. Adapted from Ref. 242 (Copyright 1999 American Chemical Society). (d) Hierarchical cluster analysis from the average Raman spectra of three yeast cells types. Adapted from Ref. 260 (Copyright 2005 Wiley–Liss, Inc). (e) 2-D and 3-D PCA plots show the separation of data based on different modes of cell death. Reproduced from Ref. 209

process as it is scaled-up.<sup>261</sup> Lipids are often essential components of colloidal pharmaceuticals. Raman microscopy has proven particularly sensitive to lipids, which contain unique Raman signal producing hydrocarbon chains. Raman microscopy can determine the structure of lipids to determine the packing behaviour and phase transitions.<sup>262</sup>

#### 4.5 Forensics

Accurate forensic analysis is required by authorities for obtaining successful prosecutions. Current systems rely on electrophoretic DNA chips, which require pre-processing, filtering and polymerase chain reactions to enhance the number of DNA strands.<sup>263</sup> Alternatives to these DNA chips include optical options such as fluorescent systems, which require the use of

fluorescent tags.<sup>264,265</sup> Raman systems can also be used for DNA characterisation, providing a quick and thorough analysis of biological forensic markers. Raman analysis has been used for the forensic analysis of body fluid traces<sup>266</sup> including whole blood,<sup>267</sup> vaginal fluids,<sup>268</sup> forensic pharmaceutical investigations,<sup>269</sup> explosives<sup>6</sup> and drugs of abuse.<sup>270</sup>

Microfluidics has the potential to enhance this field, as the majority of forensic samples are organic in nature and can be suspended in liquid, allowing them to be measured in Raman-microfluidic devices. Furthermore, microfluidics provide ideal lab-on-a-chip environments, therefore sample preparation can be conducted in a fast and portable fashion. Samples of DNA and other body fluids can be stored in their liquid forms, and Raman microscopy provides a non-destructive method of testing,

allowing the sample to be re-used if required. Despite all of these benefits there are still the issues of portability and cost, which have been thoroughly discussed in the “Considerations for Raman spectroscopy in microfluidics” section. Low cost devices and access to the right data banks are required for widespread forensic analysis using Raman-microfluidic devices.

## 5. Data analysis

Analysis of data from Raman microscopy-microfluidic measurements is extremely important for gaining the correct insights regarding the samples under investigation. Raman spectroscopy data obtained from a microfluidic system is not as definitive as the information obtained from other microfluidic systems such as DNA chips. However, the Raman-microfluidic data is far more specific than most other optical analytical tools such as microfluidics integrated with light microscopy and UV-Vis absorption spectroscopy. Alternatively, fluorescence-microfluidic systems are used for the detection of specific targets with high sensitivity, however they are useful only for a limited number of predetermined targets.

Many Raman-microfluidics systems are used for bio-analytical studies. However, complex organic compounds generate a large number of Raman peaks, which are hard to distinguish and categorise. Therefore, the accurate analysis of data from such systems is an important issue. Raman data can be used not only for qualitative analysis (determining the type of materials in the microfluidics environment), but also for quantitative analysis (determining the concentration of materials). A brief comparison of the major Raman spectral data analysis techniques is presented in Table 1.

### 5.1 Qualitative analysis

Qualitative analysis focusses on Raman spectral information that describes the types of materials being detected, essentially using the chemicals optical ‘fingerprint’ to determine its presence in the microfluidic system. For simple Raman spectra, it is convenient to compare them with a known Raman spectrum to determine the correlation in terms of peak positions and relative intensities.

In microfluidics it is likely that, due to the presence of multiple chemicals, spectral data will be multivariate in character, containing Raman signatures from many components simultaneously. Wavenumber and peak intensity can be readily applied for analysing single or multiple targets, where the peaks of the different components do not overlap excessively. Analysis of multivariate data should provide researchers with statistical information about the identity and relative abundance of the analyte in the region of interest. These analysis methods are most suited to biological candidates such as proteins, amino acids, sugars, DNA, RNA, lipids and dissolved gases, where the Raman spectrum would contain peaks from a large number of chemical constituents.

There are a number of different multivariate analysis techniques that exist for determining the components of complex Raman-microfluidic spectra. These techniques are capable of extracting useful information using a variety of data-driven processes for analysing Raman-microfluidics data.

#### 5.1.1 Deconvolution of Raman spectra

Multivariate Raman spectra, such as that captured by Raman-

microfluidic systems, can be deconvolved, or broken down, into the known peaks for various Raman-active bonds. The resulting deconvolved spectra can then be analysed using direct wavelength correlation to determine its components. Two main techniques are used for the blind deconvolution of Raman spectroscopic data, the Lorentzian and Gaussian methods, which help to narrow the scope of the blind deconvolution process.<sup>242,271</sup> These two techniques have been compared against each other for the study of several proteins, where deconvolved Raman data was used to determine the effect of heat treatment on C-H bonds of the proteins (Fig. 11(a)–(c)).<sup>242</sup> Other examples where deconvolution has been used for Raman spectral analysis include the study of human tissue samples,<sup>272</sup> studies of single-wall carbon nanotube (SWCNT) exposure on mice<sup>244</sup> and prostate cancer cells.<sup>243</sup> Regarding Raman-microfluidics, this method is also able to distinguish peaks that are generated from microfluidic system materials, such as PDMS, glass, water or other solvents and even excess contaminants.

#### 5.1.2 Hierarchical cluster analysis (HCA)

HCA seeks to order a series of spectra into clusters based on a hierarchy of commonalities found in the Raman data.<sup>273</sup> This technique is used mostly for categorising biological samples, where they can be organised and identified into their types using spectral information. This technique is readily usable for Raman-microfluidic data, as constant background signals are ignored by the algorithms, which are designed to focus on the differences within the datasets. Examples of HCA for Raman data analysis include investigating and classifying single yeast cell types (Fig. 11(d)),<sup>260</sup> cells grown in different environmental media<sup>274</sup> and various bacterial samples.<sup>275</sup>

#### 5.1.3 Principal component analysis (PCA)

PCA compresses Raman spectral data into a fixed number of features (principal components), by calculating the orthogonal directions (scores), associated with the maximum variance in the Raman data. This method implies that there is a fair amount of redundant data in the Raman spectrum, as one element can contribute to many Raman bands.<sup>276</sup> Specifically for Raman-microfluidic analysis, the redundant data could be generated from contaminants in the liquids, or background signals from microchannel structures (such as PDMS and glass substrates) or ‘memory effect’ inconsistencies. The score points are then plotted against one another and used to identify trends and groups of common Raman signatures. PCA is commonly used for qualitative analysis of biological Raman-microfluidics spectra, including the analysis of coronary artery tissue,<sup>277</sup> both primary human keratinocyte and human cervical squamous carcinoma cells,<sup>87</sup> leukaemia cell life cycle states (Fig. 11(e)),<sup>209</sup> breast cancer diagnosis<sup>278</sup> and ethanol content in consumable tequila.<sup>279</sup> Other recent work has shown the application of PCA for studying the outputs of hyper-spectral Raman imaging in an effort to map the locations and intensities of specific components over the image.<sup>280</sup>

## 5.2 Quantitative analysis

Raman-microfluidic data is capable of providing quantitative information on target materials, allowing the determination of particle sizes<sup>281</sup> and concentrations of chemical components in the target area. Such Raman-microfluidic systems can be used for the study of suspended particles with diameters between 5 and

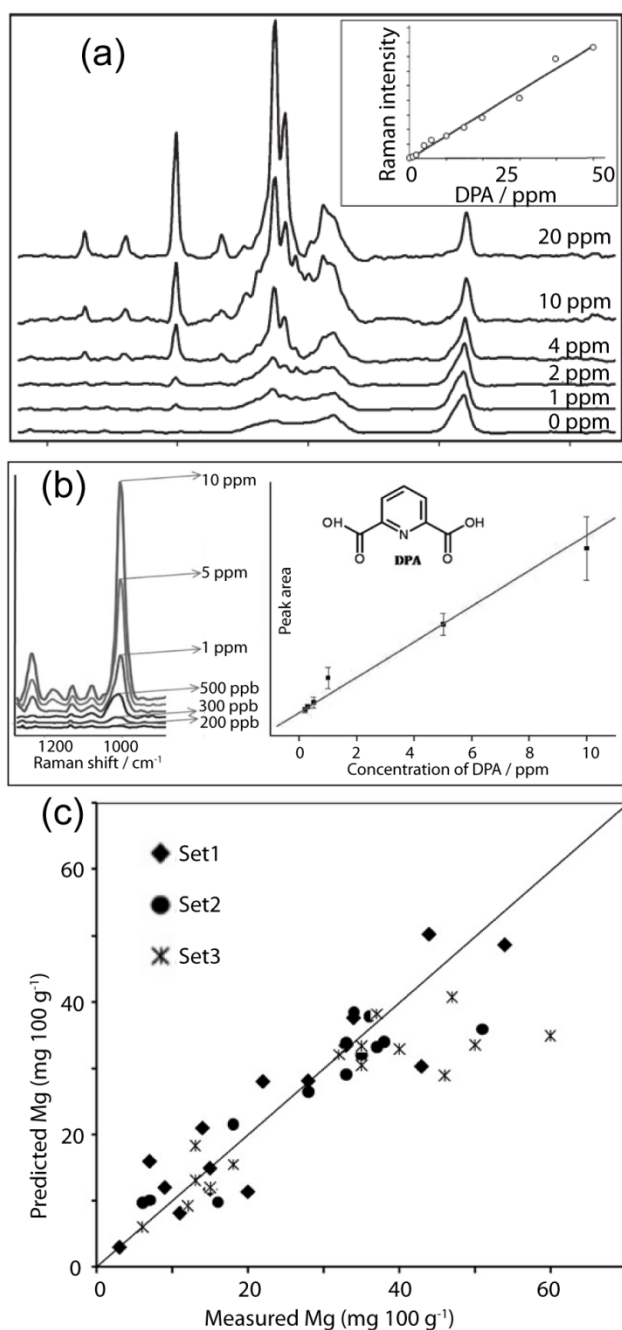


**Fig. 12** Examples of quantitative evaluation using Raman microscopic data. (a) SERS spectra of varying concentrations of dipicolinic acid. The calibration plot obtained from the spectra is shown as an inset. Reproduced from Ref. 247. (b) Concentration-dependent SERS spectra of dipicolinic acid ranging from 100 ppb to 10 ppm using the SERS peak intensity at 1005  $\text{cm}^{-1}$ . Reproduced from Ref. 136. (c) PLS prediction of magnesium (Mg) content of soil samples. Reproduced from Ref. 282 (Copyright (2010), with permission from Elsevier)

50 nm, where it is possible to determine their size by using the broadening characteristic of certain Raman peaks.<sup>281,283-285</sup> Other examples for diamond structures use Raman peak shifts for determining sizes between 0.1 and 2 nm<sup>286,287</sup> or to determine the strain on a particular bond.<sup>288</sup>

For quantitative measurements of concentration, it is common to use methods such as regression analysis, where the concentration of the sample is measured using the intensity

and/or area of Raman peaks. Regression analysis creates an analytical relationship between the known concentration values and the Raman spectral data. Once the concentration relationships have been determined it becomes possible to assess the concentration of an unknown sample. Raman-microfluidic analysis which implement this technique to determine concentration include analytes such as dipicolinic acid (Fig. 12(a) – (b)),<sup>136,247</sup> promethazine,<sup>60</sup> mitoxantrone<sup>60</sup> and glucose.<sup>248,249</sup>

Quantitative analysis of several components simultaneously, especially when these components have overlapping Raman peaks, can be a complex issue. However, this is a scenario that is commonly seen in many Raman-microfluidics measurements where contaminants and interfering reagents exist. There is always a trade-off between the number of pre-processing stages for purification of samples and the complexity of the quantitative analysis. Obviously a high degree of qualitative analysis is also included in determining the quantities of chemicals in complex systems, especially in Raman-microfluidic systems as these are multivariate in nature and require some form of statistical analysis.

Partial least squares (PLS) is a multivariate regression technique where a set of known (expected) chemicals is compared against a complex spectrum in order to extract a linear relationship between the known concentration of a particular component and the intensity of Raman-microfluidic spectral information. As PLS requires prior knowledge of the target chemicals it is usually coupled with a qualitative technique, such as PCA, for determining the presence of any target chemicals. PLS has been used in analysing the data from Raman-microfluidic systems for the detection of glucose, lactic acid and creatinine at various concentrations (Fig. 12(c)–(e)).<sup>126</sup> Further examples include the analysis of mass fractions of  $\text{Ba}(\text{NO}_3)_2$ ,<sup>289</sup> concentrations of oxytetracycline<sup>231</sup> and sample fractions of carbon, magnesium, sodium and potassium from soil samples.<sup>282</sup>

Principal component recognition (PCR) is a multivariate quantification technique that is, in some ways, is similar to PLS. PCR uses the principal components of the Raman data to generate the linear concentration relationships, as opposed to the expected chemical specific information used in PLS strategies. PCR requires the calculation of principal components, similar to PCA, and also assumes the presence of redundant data in the Raman-microfluidic spectra, such as data from contaminants or microchannel structure materials (e.g. PDMS or glass). Unlike PLS, this method does not require the Raman signature of the target chemical, as it uses the principal component. However, this fact also makes PCR analysis less stable for determining concentration behaviour, as the principal component may not only contain Raman information from the desired material, but also information from other materials. Nevertheless, PCR has been widely used for determining quantitative data from Raman-microfluidic spectra in examples such as thermoplastic polyurethane analysis,<sup>241</sup> preeclampsia (gestational hypertension) studies,<sup>233</sup> identification of medicine counterfeits,<sup>234</sup> laryngeal cancer diagnosis<sup>236</sup> and for the study of saliva from lung cancer patients.<sup>235</sup>

## 6. Other vibrational spectroscopy techniques in microfluidics

Vibrational spectroscopic methods, other than Raman spectroscopy, have been employed for the purpose of chemical and biological analysis in microfluidics. Such methods have increasingly been used to probe both continuous and segmented microfluidic systems in the past few years. Of these vibrational methods, FTIR is the most commonly implemented technique, where a broadband IR source illuminates a sample and the resulting transmitted light is studied (either absorption or transmission spectral information can be used). The light which is transmitted or absorbed by the sample forms spectroscopic patterns relating to the types and absorption strengths of bonds (mostly asymmetrical bonds) present within in the target materials. This information allows characteristic moieties of the molecular structure to be identified. FTIR can be used for characterisation of complex and, in particular, biological samples in microfluidics.<sup>230</sup>

Alternatively, attenuated total reflection infrared (ATR-IR) spectroscopic imaging is suitable for samples where transmission FTIR is impractical. ATR-IR uses a high refractive index crystal that allows IR radiation to reflect within the ATR crystal several times. The resulting evanescent wave penetrates the samples to depths on the order of 1  $\mu\text{m}$ .<sup>290</sup> In terms of spectral content, this method is comparable to transmission FTIR, providing highly detailed information regarding the chemical bonds present on the surface of target samples. There are effective demonstrations of ATR-IR integration with microfluidics for monitoring the mixing of water and reagents.<sup>291</sup>

The integration of FTIR and ATR-IR with microfluidics presents several problems, which are yet to be overcome. These vibrational methods are not ideal for probing small samples, as there is insufficient interaction of incident light when targeting small sample volumes. Hence large sample volumes that fill the field of illumination are usually required. Additionally, a specific issue for microfluidics is the fact that IR vibrational spectroscopy has a strong response to the OH bonds present in water. This can be very useful for some applications, especially for the study of oils.<sup>292</sup> However, in the context of microfluidics, water is commonly used as a solvent or the background suspending medium for materials (especially in biosensors) and as such it can be very difficult to extract the IR spectra of suspended materials from the strong OH background.

The methods for ATR-IR imaging suffer from poor penetration depths, and also require the ATR crystal to be embedded and interfaced as part of the microchannel itself. Furthermore for detecting suspended materials, it would first be necessary to position the material in direct contact with the ATR crystal so as to minimise refractive index disturbances between the crystal and the sample and provide enough sample material for analysis within its limited penetration depth.

In comparison to FTIR and ART-IR, Raman vibrational spectra are characterised by distinct sharp spectral lines, corresponding to asymmetric bonds. These peaks can be relatively easily separated from background spectra via filtering. Further, water does not produce a strong Raman response (see the “Aqueous media and microfluidics” section) and hence Raman is well suited to the analysis of aqueous solutions and small samples

suspended in water, as is often the case for microfluidics. Normal Raman spectroscopy does not require close proximity to the channel wall and is highly compatible (see the “Considerations for Raman microscopy in microfluidics” section) with confocal microscopy, allowing it to be readily used to interrogate samples at any location within a microfluidic channel. These advantages are balanced by the fact that Raman scattering is an inherently weak process, requiring careful optical concentration, selective collection, spectral filtering and post-processing of the signals in order to improve the signal-to-noise ratio. Methods to enhance Raman spectra are available, but these come at the cost of inherent trade-offs, similar to limitations of enhanced ATR-IR.

Since Raman microscopy tends to probe non-symmetrical bonds, it can provide complementary information to that discovered by FTIR. Therefore FTIR and Raman microscopy are often used together for studying complex samples, in order to obtain as much information as possible about both symmetrical and asymmetrical bonds of localised and distributed samples.<sup>293-295</sup>

## 7. Conclusion and future prospects

Raman systems provide extremely sensitive and accurate measurements, and can be utilised to study small sample volumes of interest and a large number of different materials. It is quite natural that microfluidics have been integrated with Raman microscopy, as microfluidic devices enhance the ability to accurately control fluids at very small volumes, allowing for trapping, sorting, measuring and culturing or reacting materials and chemicals. The integration of these two technologies has generated a large amount of research, with applications in pharmacology, forensics and bioanalytics. Furthermore, sophisticated data analysis methods have been shown to improve the utility of Raman-microfluidics data where deconvolution, PCA, HCA and other multivariate analysis methods can expand the usefulness of current systems to allow for true multiplexing of analytes, and even enable the analysis of entire biological systems such as cells and other micro-organisms.

The flexibility and diverse capabilities of Raman-microfluidic systems are producing a rapid growth in the popularity of this technique across a wide range of fields. These systems will attract more users for applications in health and safety, diagnostics, industrial processes, pharmaceuticals, forensics, food and quality control, to name just a few.

Microfluidic units are already low cost. Fortunately, the cost of Raman micro-systems is also reducing, with spectrometers becoming progressively less expensive, more sensitive, and smaller in size. It is envisaged that on-chip Raman spectrometers will be available on the market within the next decade. With the improved affordability of Raman systems, and the cost effective fabrication of microfluidic devices, it is envisioned that compact Raman-microfluidic systems will be widespread for both commercial and private use. Raman analysis may be used for quality control in industries dealing with fluids such as milk, beverages, water, oils and other liquids. Low-cost Raman microfluidics may even be introduced in systems operated by smart phones. Such systems could assist individual users with the determination of unknown liquid samples or could be used as accurate personal health monitors.

However, improvements are still needed for data analysis. The systems need to be able to break down the results from complex mixtures of biological samples commonly found at crime scenes, body fluids, food and water. The fine tuning of Raman analysis techniques will ultimately allow for the true multiplexing of material detection, in particular the real time analysis of complex biological materials. Suitable numerical analytical techniques can open up the applications of Raman-microfluidic systems for use in medical monitoring of patients, real-time monitoring of blood and saliva, studies on the effect of drugs and other compounds on organisms and even environmental monitoring. To achieve this more effectively, “libraries” of standardised Raman spectra for many common samples must be established, similar to those that exist already for X-Ray diffraction and FTIR spectra. Furthermore, the continued development of microfluidic technology along with low-cost robust optical and spectroscopic integration will enable re-usable and long-lifetime Raman microfluidic hardware that can be mass-deployed for monitoring across the full range of biological, biomedical, industrial and environmental applications of the devices.

## Notes and references

<sup>a</sup> School of Electrical and Computer Engineering, RMIT University, 124 LaTrobe St, Melbourne, Australia. Fax: +61 3 9925 2007; Tel: +61 9925 3254; E-mail: af.chrimes@ieee.org

<sup>b</sup> Faculty of Engineering and Industrial Sciences, Swinburne University of Technology, Glenferrie Rd, Hawthorn, Australia. Fax: +61 3 9214 5160; Tel: +61 3 9214 5839; E-mail: pstoddart@swin.edu.au

1. C. V. Raman and K. S. Krishnan, *Nature*, 1928, **121**, 501-502.
2. D. Drescher and J. Kneipp, *Chem. Soc. Rev.*, 2012, **41**, 5780-5799.
3. P. Matousek, *Chem. Soc. Rev.*, 2007, **36**, 1292-1304.
4. R. J. H. Clark, *Chem. Soc. Rev.*, 1995, **24**, 187-196.
5. P. Ashok and K. Dholakia, in *Optical Nano- and Microsystems for Bioanalytics*, eds. W. Fritzsche and J. Popp, Springer, Berlin Heidelberg, 2012, vol. 10, pp. 247-268.
6. K. Buckley and P. Matousek, in *Infra. Raman Spec. For. Sci.*, John Wiley & Sons, Ltd, 2012, pp. 289-294.
7. V. Otieno-Alego, *Science Access*, **2**, 492-493.
8. P. Vandenabeele, J. Tate and L. Moens, *Anal. Bioanal. Chem.*, 2007, **387**, 813-819.
9. P. Vandenabeele, B. Wehling, L. Moens, H. Edwards, M. De Reu and G. Van Hooydonk, *Anal. Chim. Acta*, 2000, **407**, 261-274.
10. J. West, M. Becker, S. Tombrink and A. Manz, *Anal. Chem.*, 2008, **80**, 4403-4419.
11. C. Zhang and D. Xing, *Chem. Rev.*, 2010, **110**, 4910-4947.
12. H. Chandra, P. J. Reddy and S. Srivastava, *Expert Rev. Proteomics*, 2011, **8**, 61-79.
13. T.-C. Chao and A. Ros, *J. R. Soc., Interface*, 2008, **5**, S139-S150.
14. J. Mairhofer, K. Roppert and P. Ertl, *Sensors*, 2009, **9**, 4804-4823.
15. R. Gupta, B. Bastani, N. J. Goddard and B. Grieve, *Analyst*, 2013, **138**, 307-314.
16. A. C. Sabuncu, J. Zhuang, J. F. Kolb and A. Beskok, *Biomicrofluid.*, 2012, **6**, 034103-034115.
17. F. Adar, M. Delhaye and E. DaSilva, *J. Chem. Educ.*, 2007, **84**, 50.
18. M. Fleischmann, P. J. Hendra and A. J. McQuillan, *Chem. Phys. Lett.*, 1974, **26**, 163-166.
19. J. Kneipp, H. Kneipp, A. Rajadurai, R. W. Redmond and K. Kneipp, *J. Raman Spectrosc.*, 2009, **40**, 1-5.
20. L. Tong, T. Zhu and Z. Liu, *Chem. Soc. Rev.*, 2011, **40**, 1296-1304.
21. K. Kneipp, M. Moskovits and H. Kneipp, *Surface-enhanced raman scattering: physics and applications*, Springer, 2006.
22. L. Guerrini and D. Graham, *Chem. Soc. Rev.*, 2012, **41**, 7085-7107.
23. L. Rodriguez-Lorenzo, L. Fabris and R. A. Alvarez-Puebla, *Anal. Chim. Acta*, 2012, **745**, 10-23.
24. D. L. Jeanmaire and R. P. Van Duyne, *J. Electroanal. Chem. Interfacial Electrochem.*, 1977, **84**, 1-20.
25. B. D. Piorek, S. J. Lee, J. G. Santiago, M. Moskovits, S. Banerjee and C. D. Meinhardt, in *PNAS*, 2007, vol. 104, pp. 18898-18901.
26. D. Pristiniski, S. L. Tan, M. Erol, H. Du and S. Sukhishvili, *J. Raman Spectrosc.*, 2006, **37**, 762-770.
27. K. R. Strehle, D. Cialla, P. Rosch, T. Henkel, M. Kohler and J. Popp, *Anal. Chem.*, 2007, **79**, 1542-1547.
28. M. Knauer, N. Ivleva, R. Niessner and C. Haisch, *Anal. Bioanal. Chem.*, 2012, **402**, 2663-2667.
29. K.-h. Yea, S. Lee, J. B. Kyong, J. Choo, E. K. Lee, S.-W. Joo and S. Lee, *Analyst*, 2005, **130**, 1009-1011.
30. A. F. Chrimes, K. Khoshmanesh, P. R. Stoddart, A. A. Kayani, A. Mitchell, H. Daima, V. Bansal and K. Kalantar-zadeh, *Anal. Chem.*, 2012, **84**, 4029-4035.
31. J. Godin, C.-H. Chen, S. H. Cho, W. Qiao, F. Tsai and Y.-H. Lo, *J. Biophotonics*, 2008, **1**, 355-376.
32. L. Chen and J. Choo, *Electrophoresis*, 2008, **29**, 1815-1828.
33. W. Siebrand and M. Z. Zgierski, *The Journal of Chemical Physics*, 1979, **71**, 3561-3569.
34. M. Kakita, V. Kaliaperumal and H.-o. Hamaguchi, *J. Biophotonics*, 2012, **5**, 20-24.
35. R. Chao, R. Khanna and E. Lippincott, *J. Raman Spectrosc.*, 1975, **3**, 121-131.
36. F. Bonhomme, J.-L. Bruneel and L. Thouin, *J. Electroanal. Chem.*, 2000, **484**, 1-17.
37. F. T. Docherty, P. B. Monaghan, R. Keir, D. Graham, W. E. Smith and J. M. Cooper, *Chem. Commun.*, 2004, **1**, 118-119.
38. D. Graham and K. Faulds, *Chem. Soc. Rev.*, 2008, **37**, 1042-1051.
39. K. Kneipp, Y. Wang, R. R. Dasari and M. S. Feld, *Appl. Spectrosc.*, 1995, **49**, 780-784.
40. R. Keir, E. Igata, M. Arundell, W. E. Smith, D. Graham, C. McHugh and J. M. Cooper, *Anal. Chem.*, 2002, **74**, 1503-1508.
41. R. Begley, A. Harvey and R. L. Byer, *Appl. Phys. Lett.*, 1974, **25**, 387-390.
42. A. Wipfler, T. Buckup and M. Motzkus, *Appl. Phys. Lett.*, 2012, **100**, 071102:071102-071104.
43. M. Lütgens, S. Chatzipapadopoulos and S. Lochbrunner, *Opt. Express*, 2012, **20**, 6478-6487.
44. C. L. Evans and X. S. Xie, *Annu. Rev. Anal. Chem.*, 2008, **1**, 883-909.
45. C. W. Freudiger, W. Min, B. G. Saar, S. Lu, G. R. Holtom, C. He, J. C. Tsai, J. X. Kang and X. S. Xie, *Science*, 2008, **322**, 1857-1861.
46. J. Stadler, T. Schmid and R. Zenobi, *Nanoscale*, 2012, **4**, 1856-1870.
47. P. Hermann, A. Hermelink, V. Lausch, G. Holland, L. Möller, N. Bannert and D. Naumann, *Analyst*, 2011, **136**, 1148-1152.
48. H. Kim, K. M. Kosuda, R. P. Van Duyne and P. C. Stair, *Chem. Soc. Rev.*, 2010, **39**, 4820-4844.
49. M. J. Higgins, T. Fukuma and S. P. Jarvis, *Imaging & Microscopy*, 2006, **8**, 47-50.
50. C. L. Smith, in *Current Protocols in Microbiology*, John Wiley & Sons, Inc., 2005.
51. T. Park, S. Lee, G. H. Seong, J. Choo, E. K. Lee, Y. S. Kim, W. H. Ji, S. Y. Hwang and D. G. Gweon, *Lab Chip*, 2005, **5**, 437-442.
52. G. Kostovski, D. White, A. Mitchell, M. Austin and P. Stoddart, *Biosens. Bioelectron.*, 2009, **24**, 1531-1535.
53. M. Ghomi, *Advances in Biomedical Spectroscopy*, IOS Press, Amsterdam, 2012.
54. Y. Ward, R. J. Young and R. A. Shatwell, *J. Appl. Phys.*, 2007, **102**, 023512-023517.
55. A. D. McFarland, M. A. Young, J. A. Dieringer and R. P. Van Duyne, *J. Phys. Chem. B*, 2005, **109**, 11279-11285.
56. J. Enger, M. Goksor, K. Ramser, P. Hagberg and D. Hanstorp, *Lab Chip*, 2004, **4**, 196-200.
57. K. König, H. Liang, M. Berns and B. Tromberg, *Opt. Lett.*, 1996, **21**, 1090-1092.

58. K. Ramser, J. Enger, M. Goksor, D. Hanstorp, K. Logg and M. Kall, *Lab Chip*, 2005, **5**, 431-436.
59. P. Yi, A. A. Kayani, A. F. Chrimes, K. Ghorbani, S. Nahavandi, K. Kalantar-zadeh and K. Khoshmanesh, *Lab Chip*, 2012, **12**, 2520-2525.
60. K. R. Ackermann, T. Henkel and J. Popp, *ChemPhysChem*, 2007, **8**, 2665-2670.
61. A. März, K. R. Ackermann, D. Malsch, T. Bocklitz, T. Henkel and J. Popp, *J. Biophotonics*, 2009, **2**, 232-242.
62. G. Wang, C. Lim, L. Chen, H. Chon, J. Choo, J. Hong and A. J. deMello, *Anal. Bioanal. Chem.*, 2009, **394**, 1827-1832.
63. S. L. Gras, T. Mahmud, G. Rosengarten, A. Mitchell and K. Kalantar-zadeh, *ChemPhysChem*, 2007, **8**, 2036-2050.
64. H. Rong, Y.-H. Kuo, S. Xu, A. Liu, R. Jones, M. Paniccia, O. Cohen and O. Raday, *Opt. Express*, 2006, **14**, 6705-6712.
65. H. Rong, S. Xu, Y.-H. Kuo, V. Sih, O. Cohen, O. Raday and M. Paniccia, *Nat. Photon.*, 2007, **1**, 232-237.
66. P. C. Ashok, G. P. Singh, H. A. Rendall, T. F. Krauss and K. Dholakia, *Lab Chip*, 2011, **11**, 1262-1270.
67. S. Dochow, C. Krafft, U. Neugebauer, T. Bocklitz, T. Henkel, G. Mayer, J. Albert and J. Popp, *Lab Chip*, 2011, **11**, 1484-1490.
68. P. R. Stoddart and D. J. White, *Anal. Bioanal. Chem.*, 2009, **394**, 1761-1774.
69. H. C. Hunt and J. S. Wilkinson, *Opt. Express*, 2012, **20**, 9442-9457.
70. I. R. Lewis and H. G. M. Edwards, *Handbook of Raman Spectroscopy: From the Research Laboratory to the Process Line*, Taylor & Francis, 2001.
71. R. J. Nemanich, C. C. Tsai and G. A. N. Connell, *Phys. Rev. Lett.*, 1980, **44**, 273-276.
72. A. F. Chrimes, A. Kayani, K. Khoshmanesh and K. Kalantar-zadeh, in *SPIE Micro- and Nanotechnology Sensors, Systems, and Applications*, eds. T. George, M. S. Islam and A. K. Dutta, Boston, USA, 2011, vol. 8031.
73. M. Dieterle and G. Mestl, *Phys. Chem. Chem. Phys.*, 2002, **4**, 822-826.
74. J. P. Baltrus, L. E. Makovsky, J. M. Stencel and D. M. Hercules, *Anal. Chem.*, 1985, **57**, 2500-2503.
75. I. E. Wachs and C. A. Roberts, *Chem. Soc. Rev.*, 2010, **39**, 5002-5017.
76. Y. Y. Wang, Z. H. Ni, Z. X. Shen, H. M. Wang and Y. H. Wu, *Appl. Phys. Lett.*, 2008, **92**, 043121-043123.
77. D. H. Shin, J.-E. Kim, H. C. Shim, J.-W. Song, J.-H. Yoon, J. Kim, S. Jeong, J. Kang, S. Baik and C.-S. Han, *Nano Lett.*, 2008, **8**, 4380-4385.
78. B.-H. Jun, M. S. Noh, G. Kim, H. Kang, J.-H. Kim, W.-J. Chung, M.-S. Kim, Y.-K. Kim, M.-H. Cho and D. H. Jeong, *Anal. Biochem.*, 2009, **391**, 24-30.
79. K. Badizadegan, V. Backman, C. W. Boone, C. P. Crum, R. R. Dasari, I. Georgakoudi, K. Keefe, K. Munger, S. M. Shapshay and E. E. Sheets, *Faraday Discuss.*, 2003, **126**, 265-279.
80. I. J. Bigio and S. G. Bown, *Cancer Biol. Ther.*, 2004, **3**, 259-267.
81. J. Hung, S. Lam, J. C. Leriche and B. Palcic, *Lasers Surg. Med.*, 1991, **11**, 99-105.
82. N. Stone, C. Kendall, N. Shepherd, P. Crow and H. Barr, *J. Raman Spectrosc.*, 2002, **33**, 564-573.
83. N. Stone, C. Kendall, J. Smith, P. Crow and H. Barr, *Faraday Discuss.*, 2003, **126**, 141-157.
84. I. Nabiev, H. Morjani and M. Manfait, *Eur. Biophys. J.*, 1991, **19**, 311-316.
85. A. Sujith, T. Itoh, H. Abe, K. I. Yoshida, M. S. Kiran, V. Biju and M. Ishikawa, *Anal. Bioanal. Chem.*, 2009, **394**, 1803-1809.
86. A. Sujith, T. Itoh, H. Abe, A. A. Anas, K. Yoshida, V. Biju and M. Ishikawa, *Appl. Phys. Lett.*, 2008, **92**, 103901:103901-103903.
87. P. R. T. Jess, V. Garcés-Chávez, D. Smith, M. Mazilu, L. Paterson, A. Riches, C. S. Herrington, W. Sibbett and K. Dholakia, *Opt. Express*, 2006, **14**, 5779-5791.
88. P. W. Loeffen, G. Maskall, S. Bonthron, M. Bloomfield, C. Tombling and P. Matousek, *Optical Materials in Defence Systems Technology VIII*, Prague, Czech Republic, 2011.
89. M. Galvin and D. Zerulla, *ChemPhysChem*, 2011, **12**, 913-914.
90. R. Lall, T. J. Donohue, S. Marino and J. C. Mitchell, *Mathematical and Computer Modelling*, 2011, **53**, 1363-1373.
91. K. Egashira and N. Nishi, *J. Phys. Chem. B*, 1998, **102**, 4054-4057.
92. J. F. Mammone, S. K. Sharma and M. Nicol, *J. Phys. Chem.*, 1980, **84**, 3130-3134.
93. D. Mark, S. Haeberle, G. Roth, F. von Stetten and R. Zengerle, *Chem. Soc. Rev.*, 2010, **39**, 1153-1182.
94. T. Tsukahara, K. Mawatari and T. Kitamori, *Chem. Soc. Rev.*, 2010, **39**, 1000-1013.
95. B. H. Jo, L. M. Van Lerberghe, K. M. Motsegood and D. J. Beebe, *Microelectromechanical Systems, Journal of*, 2000, **9**, 76-81.
96. S. Marre and K. F. Jensen, *Chem. Soc. Rev.*, 2010, **39**, 1183-1202.
97. A. Lenshof and T. Laurell, *Chem. Soc. Rev.*, 2010, **39**, 1203-1217.
98. R. C. Anderson, G. J. Bogdan, Z. Bamiv, T. D. Dawes, J. Winkler and K. Roy, *International Conference on Solid State Sensors and Actuators*, Chicago, 1997.
99. Y. Xia and G. M. Whitesides, *Annu. Rev. Mater. Sci.*, 1998, **28**, 153-184.
100. N. Liu, C. Aymonier, C. Lecoutre, Y. Garrabos and S. Marre, *Chem. Phys. Lett.*, 2012, **551**, 139-143.
101. P. Abgrall, V. Conedera, H. Camon, A. M. Gue and N. T. Nguyen, *Electrophoresis*, 2007, **28**, 4539-4551.
102. J. S. Kuo and D. T. Chiu, *Lab Chip*, 2011, **11**, 2656-2665.
103. S. K. Sia and G. M. Whitesides, *Electrophoresis*, 2003, **24**, 3563-3576.
104. P. Kim, K. W. Kwon, M. C. Park, S. H. Lee, S. M. Kim and K. Y. Suh, *BioChip J.*, 2008, **2**, 1-11.
105. P. S. Dittrich, K. Tachikawa and A. Manz, *Anal. Chem.*, 2006, **78**, 3887-3907.
106. K. Ohno, K. Tachikawa and A. Manz, *Electrophoresis*, 2008, **29**, 4443-4453.
107. G. S. Fiorini and D. T. Chiu, *BioTechniques*, 2005, **38**, 429-446.
108. A. F. Chrimes, A. A. Kayani, K. Khoshmanesh, P. R. Stoddart, P. Mulvaney, A. Mitchell and K. Kalantar-zadeh, *Lab Chip*, 2011, **11**, 921-928.
109. A. Rasmussen, C. Mavriplis, M. Zaghoul, O. Mikulchenko and K. Mayaram, *Sens. Actuators, A*, 2001, **88**, 121-132.
110. V. Lien and F. Vollmer, *Lab Chip*, 2007, **7**, 1352-1356.
111. I. Etchart, H. Chen, P. Dryden, J. Jundt, C. Harrison, K. Hsu, F. Marty and B. Mercier, *Sens. Actuators, A*, 2008, **141**, 266-275.
112. C. Gosse, C. Bergaud and P. Löw, in *Thermal Nanosystems and Nanomaterials*, ed. S. Volz, Springer Berlin Heidelberg, 2009, vol. 118, pp. 301-341.
113. M. A. Murrnan and H. Najjaran, *Lab Chip*, 2012, **12**, 2053-2059.
114. J. Collins and A. P. Lee, *Lab Chip*, 2003, **4**, 7-10.
115. S. Seo, T. Stintzing, I. Block, D. Pavlidis, M. Rieke and P. G. Layer, *Microwave Symposium Digest*, 2008 IEEE MTT-S International, 2008.
116. A. A. Kayani, A. F. Chrimes, K. Khoshmanesh, K. Kalantar-zadeh and A. Mitchell, in *Micro- and Nanotechnology Sensors, Systems, and Applications Iii - SPIE*, eds. T. George, M. S. Islam and A. K. Dutta, 2011, vol. 8031.
117. A. A. Kayani, K. Khoshmanesh, S. A. Ward, A. Mitchell and K. Kalantar-zadeh, *Biomicrofluid.*, 2012, **6**, 031501-031532.
118. A. P. Lee, M. V. Patel, A. R. Tovar and Y. Okabe, *Jala*, 2010, **15**, 449-454.
119. A. Lee and M. Patel, *J. Acoust. Soc. Am.*, 2012, **132**, 1953-1953.
120. M. V. Patel, A. R. Tovar and A. P. Lee, *Lab Chip*, 2012, **12**, 139-145.
121. M. M. Miller, P. E. Sheehan, R. L. Edelstein, C. R. Tamanaha, L. Zhong, S. Bounnak, L. J. Whitman and R. J. Colton, *J. Magn. Magn. Mater.*, 2001, **225**, 138-144.
122. G. Kostovski, D. J. White, A. Mitchell, M. W. Austin and P. R. Stoddart, *Biosens. Bioelectron.*, 2009, **24**, 1531-1535.
123. T. Yasui, Y. Omoto, K. Osato, N. Kaji, N. Suzuki, T. Naito, Y. Okamoto, M. Tokeshi, E. Shamoto and Y. Baba, *Anal. Sci.*, 2012, **28**, 57-57.
124. I. Mitsuhsisa, S. Keita, K. Shinya, K. Yasuhiro, S. Yohei and H. Koichi, *J. Micromech. Microeng.*, 2012, **22**, 065023.
125. B. Kuswandi, Nuriman, J. Huskens and W. Verboom, *Anal. Chim. Acta*, 2007, **601**, 141-155.

126. A. J. Berger, Y. Wang and M. S. Feld, *Appl. Opt.*, 1996, **35**, 209-212.
127. D. J. Laser and J. G. Santiago, *J. Micromech. Microeng.*, 2004, **14**, R35.
128. T. M. Squires and S. R. Quake, *Rev. Mod. Phys.*, 2005, **77**, 977.
129. A. van Dintther, C. Schroën, F. Vergeldt, R. van der Sman and R. Boom, *Adv. Colloid Interface Sci.*, 2012, **173**, 23-34.
130. C. Y. Lee, C. L. Chang, Y. N. Wang and L. M. Fu, *Int. J. Mol. Sci.*, 2011, **12**, 3263-3287.
131. T. H. Schulte, R. L. Bardell and B. H. Weigl, *Clin. Chim. Acta*, 2002, **321**, 1-10.
132. A. E. Kamholz and P. Yager, *Biophys. J.*, 2001, **80**, 155-160.
133. R. F. Ismagilov, D. Rosmarin, P. J. A. Kenis, D. T. Chiu, W. Zhang, H. A. Stone and G. M. Whitesides, *Anal. Chem.*, 2001, **73**, 4682-4687.
134. Z. Nie, S. Xu, M. Seo, P. C. Lewis and E. Kumacheva, *J. Am. Chem. Soc.*, 2005, **127**, 8058-8063.
135. J. Wagner and J. M. Köhler, *Nano Lett.*, 2005, **5**, 685-691.
136. L. X. Quang, C. Lim, G. H. Seong, J. Choo, K. J. Do and S. K. Yoo, *Lab Chip*, 2008, **8**, 2214-2219.
137. N. T. Nguyen, *Micromixers: Fundamentals, Design, and Fabrication*, Elsevier Science, 2008.
138. A. Y. Lau, L. P. Lee and J. W. Chan, *Lab Chip*, 2008, **8**, 1116-1120.
139. J. R. Moffitt, Y. R. Chemla, S. B. Smith and C. Bustamante, *Annu. Rev. Biochem.*, 2008, **77**, 205-228.
140. O. G. Helleso, P. Lovhaugen, A. Z. Subramanian, J. S. Wilkinson and B. S. Ahluwalia, *Lab Chip*, 2012, **12**, 3436-3440.
141. H. Liang, K. T. Vu, P. Krishnan, T. C. Trang, D. Shin, S. Kimel and M. W. Berns, *Biophys. J.*, 1996, **70**, 1529-1533.
142. G. P. Singh, G. Volpe, C. M. Creely, H. Grottsch, I. M. Geli and D. Petrov, *J. Raman Spectrosc.*, 2006, **37**, 858-864.
143. G. Thalhammer, R. Steiger, S. Bernet and M. Ritsch-Marte, *J. Opt.*, 2011, **13**, 044024.
144. L. M. Tong, V. D. Miljkovic and M. Kall, in *Optical Trapping and Optical Micromanipulation VII*, eds. K. Dholakia and G. C. Spalding, Spie-Int Soc Optical Engineering, Bellingham, 2010, vol. 7762.
145. C. G. Xie, M. A. Dinno and Y. Q. Li, *Opt. Lett.*, 2002, **27**, 249-251.
146. C. G. Xie and Y. Q. Li, *Appl. Phys. Lett.*, 2002, **81**, 951-953.
147. C. G. Xie and Y. Q. Li, *J. Appl. Phys.*, 2003, **93**, 2982-2986.
148. L. Tong, K. Ramser and M. Käll, in *Raman Spectroscopy for Nanomaterials Characterization*, ed. C. S. R. Kumar, Springer Berlin Heidelberg, 2012, pp. 507-530.
149. W.-H. Tan and S. Takeuchi, *PNAS*, 2007, **104**, 1146-1151.
150. P. J. Lee, N. C. Helman, W. A. Lim and P. J. Hung, *BioTechniques*, 2008, **44**, 91-95.
151. K. Khoshmanesh, S. Nahavandi, S. Baratchi, A. Mitchell and K. Kalantar-zadeh, *Biosens. Bioelectron.*, 2011, **26**, 1800-1814.
152. C. Zhang, K. Khoshmanesh, A. Mitchell and K. Kalantar-zadeh, *Anal. Bioanal. Chem.*, 2010, **396**, 401-420.
153. Z. D. Sandlin, M. Shou, J. G. Shackman and R. T. Kennedy, *Anal. Chem.*, 2005, **77**, 7702-7708.
154. M. B. Fox, D. C. Esveld, A. Valero, R. Lutttge, H. C. Mastwijk, P. V. Bartels, A. Berg and R. M. Boom, *Anal. Bioanal. Chem.*, 2006, **385**, 474-485.
155. N. M. Jesús-Pérez and B. H. Lapizco-Encinas, *Electrophoresis*, 2011, **32**, 2331-2357.
156. B. H. Lapizco-Encinas, R. V. Davalos, B. A. Simmons, E. B. Cummings and Y. Fintschenko, *J. Microbiol. Methods*, 2005, **62**, 317-326.
157. C. Zhang, K. Khoshmanesh, F. J. Tovar-Lopez, A. Mitchell, W. Wlodarski and K. Kalantar-zadeh, *Micro. Nano. Fluid.*, 2009, **7**, 633-645.
158. K. Khoshmanesh, S. Baratchi, F. Tovar-Lopez, S. Nahavandi, D. Wlodkowic, A. Mitchell and K. Kalantar-zadeh, *Micro. Nano. Fluid.*, 2012, **12**, 597-606.
159. C. L. Asbury, A. H. Diercks and G. van den Engh, *Electrophoresis*, 2002, **23**, 2658-2666.
160. T. Kano, T. Inaba, G. Ye and N. Miki, *J. Micro-Nano Mech.*, 2012, **7**, 61-68.
161. L. Miccio, P. Memmolo, S. Grilli and P. Ferraro, *Lab Chip*, 2012, **12**, 4449-4454.
162. A. Salmanzadeh, H. Kittur, M. B. Sano, P. C. Roberts, E. M. Schmelz and R. V. Davalos, *Biomicrofluid.*, 2012, **6**, 024104:024104-024113.
163. P. D. I. Fletcher, S. J. Haswell and X. Zhang, *Electrophoresis*, 2003, **24**, 3239-3245.
164. R. M. Connatser, M. Cochran, R. J. Harrison and M. J. Sepaniak, *Electrophoresis*, 2008, **29**, 1441-1450.
165. J. Nilsson, M. Evander, B. Hammarstrom and T. Laurell, *Anal. Chim. Acta*, 2009, **649**, 141-157.
166. J. S. Jeong, J. W. Lee, C. Y. Lee, S. Y. Teh, A. Lee and K. K. Shung, *Biomed. Microdevices*, 2011, **13**, 779-788.
167. J. R. Basore and L. A. Baker, *Anal. Bioanal. Chem.*, 2012, **403**, 2077-2088.
168. F. M. Weinert, C. B. Mast and D. Braun, *Phys. Chem. Chem. Phys.*, 2011, **13**, 9918-9928.
169. A. Bhagat, H. Bow, H. Hou, S. Tan, J. Han and C. Lim, *Med Biol Eng Comput*, 2010, **48**, 999-1014.
170. B. R. Lutz, J. Chen and D. T. Schwartz, *PNAS*, 2003, **100**, 4395-4398.
171. E. Widjaja, S. Y. Teh and M. Garland, *Appl. Spectrosc.*, 2012, **66**, 1226-1232.
172. S. Fiedler, S. G. Shirley, T. Schnelle and G. Fuhr, *Anal. Chem.*, 1998, **70**, 1909-1915.
173. L. Campagnolo, M. Nikolić, J. Perchoux, Y. L. Lim, K. Bertling, K. Loubière, L. Prat, A. D. Rakić and T. Bosch, *Micro. Nano. Fluid.*, 2012, 1-7.
174. S.-A. Leung, R. F. Winkle, R. C. R. Wootton and A. J. deMello, *Analyst*, 2005, **130**, 46-51.
175. K. C. Bantz, A. F. Meyer, N. J. Wittenberg, H. Im, O. Kurtulus, S. H. Lee, N. C. Lindquist, S. H. Oh and C. L. Haynes, *Phys. Chem. Chem. Phys.*, 2011, **13**, 11551-11567.
176. E. Hao and G. C. Schatz, *J. Chem. Phys.*, 2004, **120**, 357-366.
177. D. A. Zwemer, C. V. Shank and J. E. Rowe, *Chem. Phys. Lett.*, 1980, **73**, 201-204.
178. A. Otto and M. Futamata, in *Surface-Enhanced Raman Scattering*, eds. K. Kneipp, M. Moskovits and H. Kneipp, Springer Berlin Heidelberg, 2006, vol. 103, pp. 147-182.
179. R. M. Connatser, L. A. Riddle and M. J. Sepaniak, *J. Sep. Sci.*, 2004, **27**, 1545-1550.
180. Q. Ramadan and M. M. Gijs, *Micro. Nano. Fluid.*, 2012, **13**, 529-542.
181. S. Nitahara, M. Maeki, H. Yamaguchi, K. Yamashita, M. Miyazaki and H. Maeda, *Analyst*, 2012, **137**, 5730-5735.
182. J. W. Chan, H. Winhold, S. M. Lane and T. Huser, *Selected Topics in Quantum Electronics, IEEE Journal of*, 2005, **11**, 858-863.
183. M. G. Soler and F. Qu, in *Raman Spectroscopy for Nanomaterials Characterization*, ed. C. S. R. Kumar, Springer Berlin Heidelberg, 2012, pp. 379-416.
184. S. M. Wells, S. D. Retterer, J. M. Oran and M. J. Sepaniak, *ACS Nano*, 2009, **3**, 3845-3853.
185. J. D. Driskell, R. J. Lipert and M. D. Porter, *J. Phys. Chem. B*, 2006, **110**, 17444-17451.
186. L. Dongjin, Y. Zhijiang, S. A. Campbell and C. Tianhong, Solid-State Sensors, Actuators and Microsystems Conference, Transducers 2011 16th International, Beijing, China, 2011.
187. S. Radel, J. Schnöller, A. Dominguez, B. Lendl, M. Gröschl and E. Benes, *Elektrotech. Inftech.*, 2008, **125**, 82-85.
188. N. Choi, K. Lee, D. W. Lim, E. K. Lee, S.-I. Chang, K. W. Oh and J. Choo, *Lab Chip*, 2012, **12**, 5160-5167.
189. P. C. Ashok and K. Dholakia, *Optical Nano-and Microsystems for Bioanalytics*, 2012, 247-268.
190. M. Çulha and S. Keskin, Plasmonics in Biology and Medicine IX, San Francisco, California, 2012.
191. B.-H. Jun, M. S. Noh, G. Kim, H. Kang, J.-H. Kim, W.-J. Chung, M.-S. Kim, Y.-K. Kim, M.-H. Cho, D. H. Jeong and Y.-S. Lee, *Anal. Biochem.*, 2009, **391**, 24-30.

192. J. Khandurina and A. Guttman, *J. Chromatogr., A*, 2002, **943**, 159-183.
193. H. Mao, P. Lv and W. Wu, Solid-State Sensors, Actuators and Microsystems Conference, Transducers 2011 16th International, Beijing, China, 2011.
- 5 194. X. Yang, C. Gu, F. Qian, Y. Li and J. Z. Zhang, *Anal. Chem.*, 2011, **83**, 5888-5894.
195. J. Zhou, K. Ren, Y. Zhao, W. Dai and H. Wu, *Anal. Bioanal. Chem.*, 2012, **402**, 1601-1609.
- 10 196. S. Gulati, V. Rouilly, X. Niu, J. Chappell, R. I. Kitney, J. B. Edell and P. S. Freemont, *J. R. Soc., Interface*, 2009, **6**, S493-S506.
197. J. Trevors and L. Masson, *Antonie van Leeuwenhoek*, 2010, **98**, 249-262.
198. D. K. Lim, A. Kumar and J. M. Nam, in *Detection of Non-Amplified Genomic DNA, Soft and Biological Matter*, Springer Science+Business Media Dordrecht, 2012, pp. 67-87.
- 15 199. L. Bissonnette and M. G. Bergeron, *Expert Rev. Mol. Diagn.*, 2006, **6**, 433-450.
200. H. Zhang, M. H. Harpster, W. C. Wilson and P. A. Johnson, *Langmuir*, 2012, **28**, 4030-4037.
- 20 201. K. K. Strelau, R. Kretschmer, R. Möller, W. Fritzsche and J. Popp, *Anal. Bioanal. Chem.*, 2010, **396**, 1381-1384.
202. F. B. Myers and L. P. Lee, *Lab Chip*, 2008, **8**, 2015-2031.
203. K. Strelau, R. Kretschmer, R. Möller, W. Fritzsche and J. Popp, *Anal. Bioanal. Chem.*, 2010, **396**, 1381-1384.
- 25 204. K. K. Strelau, K. Weber, R. Möller, W. Fritzsche and J. Popp, Biophotonics: Photonic Solutions for Better Health Care II, Brussels, Belgium, 2010.
205. S. R. Quake, *Anal. Chem.*, 2007, **79**, 8557-8563.
- 30 206. A. L. Paguirigan and D. J. Beebe, *BioEssays*, 2008, **30**, 811-821.
207. A. Valero, F. Merino, F. Wolbers, R. Lutge, I. Vermes, H. Andersson and A. van den Berg, *Lab Chip*, 2004, **5**, 49-55.
208. S. Koch, M. Dreiling, M. Gutekunst, C. Bolwien, H. Thielecke and H. Mertsching, European Conference on Biomedical Optics, 2009.
- 35 209. Y. H. Ong, M. Lim and Q. Liu, *Opt. Express*, 2012, **20**, 22158-22171.
210. S.-s. Huang, D. Chen, P. L. Pelczar, V. R. Vepachedu, P. Setlow and Y.-q. Li, *J. Bacteriol.*, 2007, **189**, 4681-4687.
211. E. Eriksson, J. Scrimgeour, A. Granéli, K. Ramser, R. Wellander, J. Enger, D. Hanstorp and M. Goksör, *J. Opt. A: Pure Appl. Opt.*, 2007, **9**, S113.
- 40 212. X. Zhang, H. Yin, J. Cooper and S. Haswell, *Anal. Bioanal. Chem.*, 2008, **390**, 833-840.
213. D. Huh, D. C. Leslie, B. D. Matthews, J. P. Fraser, S. Jurek, G. A. Hamilton, K. S. Thorneloe, M. A. McAlexander and D. E. Ingber, *Sci. Transl. Med.*, 2012, **4**, 159ra147.
- 45 214. A. M. Ghaemmaghami, M. J. Hancock, H. Harrington, H. Kaji and A. Khademhosseini, *Drug Discovery Today*, 2011, **17**, 173-181.
215. H. Andersson and A. Van Den Berg, *Lab Chip*, 2004, **4**, 98-103.
- 50 216. D. E. Ingber and G. M. Whitesides, *Lab Chip*, 2012, **12**, 2089-2090.
217. D. Huh, B. D. Matthews, A. Mammoto, M. Montoya-Zavala, H. Y. Hsin and D. E. Ingber, *Science*, 2010, **328**, 1662-1668.
218. P. Matousek, E. R. C. Draper, A. E. Goodship, I. P. Clark, K. L. Ronayne and A. W. Parker, *Appl. Spectrosc.*, 2006, **60**, 758-763.
- 55 219. M. D. Keller, S. K. Majumder and A. Mahadevan-Jansen, *Opt. Lett.*, 2009, **34**, 926-928.
220. H. Xie, R. Stevenson, N. Stone, A. Hernandez-Santana, K. Faulds and D. Graham, *Angew. Chem.*, 2012, **124**, 8637-8639.
- 60 221. P. Matousek and N. Stone, *J. Biophotonics*, 2012, DOI: 10.1002/jbio.201200141.
222. N. Stone and P. Matousek, *Cancer Res.*, 2008, **68**, 4424-4430.
223. P. J. Caspers, G. W. Lucassen and G. J. Puppels, *Biophys. J.*, 2003, **85**, 572-580.
- 65 224. N. Uzunbajakava, A. Lenferink, Y. Kraan, B. Willekens, G. Vrensen, J. Greve and C. Otto, *Biopolymers*, 2002, **72**, 1-9.
225. R. M. Jarvis and R. Goodacre, *Anal. Chem.*, 2004, **76**, 40-47.
226. S. Shanmukh, L. Jones, Y. P. Zhao, J. D. Driskell, R. A. Tripp and R. A. Dluhy, *Anal. Bioanal. Chem.*, 2008, **390**, 1551-1555.
- 70 227. K. Gaus, P. Rösch, R. Petry, K. D. Peschke, O. Ronneberger, H. Burkhardt, K. Baumann and J. Popp, *Biopolymers*, 2006, **82**, 286-290.
228. X. Lu, H. Al-Qadiri, M. Lin and B. Rasco, *Food Bioprocess Technol*, 2011, **4**, 919-935.
- 75 229. P. Y. Sacré, E. Deconinck and J. De Beer, in *Counterfeit Medicines Volume II: Detection, Identification and Analysis*, eds. P. Wang and A. Wertheimer, ILM Publications, St Albans, UK, 2012.
230. M. Polakovs, N. Mironova-Ulmane, A. Pavlenko, E. Reinholds, M. Gavare and M. Grube, *Spectroscopy*, 2012, **27**.
- 80 231. C. Xiaoyun, L. Weizi, Y. Chunmei, L. Wang and B. Minghai, Virtual Environments Human-Computer Interfaces and Measurement Systems (VECIMS), 2012 IEEE International Conference, 2012.
232. R. Szostak and S. Mazurek, *Drug Test. Anal.*, 2012, DOI: 10.1002/dta.379.
- 85 233. G. Basar, U. Parlatan, S. Seninak, T. Gunel, A. Benian and I. Kalelioglu, *Spectroscopy*, 2012, **27**, 239-252.
234. K. Dégardin, Y. Roggo, F. Been and P. Margot, *Anal. Chim. Acta*, 2011, **705**, 334-341.
- 90 235. X. Li, T. Yang, S. Lib and T. Yu, 2011.
236. K. Lin, D. L. P. Cheng and Z. Huang, *Biosens. Bioelectron.*, 2012, **35**, 213-217.
237. M. D. Hargreaves, N. A. Macleod, M. R. Smith, D. Andrews, S. V. Hammond and P. Matousek, *J. Pharm. Biomed. Anal.*, 2011, **54**, 463-468.
- 95 238. S. Mazurek and R. Szostak, *J. AOAC Int.*, 2012, **95**, 744-750.
239. O. S. Fenton, L. A. Tonge, T. H. Moot and K. A. Frederick, *Spectrosc. Lett.*, 2011, **44**, 229-234.
240. K. W. C. Poon, F. M. Lyng, P. Knief, O. Howe, A. D. Meade, J. F. Curtin, H. J. Byrne and J. Vaughan, *Analyst*, 2012, **137**, 1807-1814.
- 100 241. A. T. Weakley, P. C. T. Warwick, T. E. Bitterwolf and D. E. Aston, *Appl. Spectrosc.*, 2012, **66**, 1269-1278.
242. N. K. Howell, G. Arteaga, S. Nakai and E. C. Y. Li-Chan, *J. Agric. Food Chem.*, 1999, **47**, 924-933.
- 105 243. A. Pallaoro, G. B. Braun and M. Moskovits, *PNAS*, 2011, **108**, 16559-16564.
244. T. Ingle, E. Dervishi, A. R. Biris, T. Mustafa, R. A. Buchanan and A. S. Biris, *J. Appl. Toxicol.*, 2012, DOI: 10.1002/jat.2796.
- 110 245. L. Nikiel and P. W. Jagodzinski, *Carbon*, 1993, **31**, 1313-1317.
246. L. Ashton, L. D. Barron, B. Czarnik-Matusewicz, L. Hecht, J. Hyde and E. W. Blanch, *Mol. Phys.*, 2006, **104**, 1429-1445.
247. S. E. J. Bell, J. N. Mackle and N. M. S. Sirimuthu, *Analyst*, 2005, **130**, 545-549.
- 115 248. Z.-S. Wu, G.-Z. Zhou, J.-H. Jiang, G.-L. Shen and R.-Q. Yu, *Talanta*, 2006, **70**, 533-539.
249. X. Yang, A. Zhang, D. Wheeler, T. Bond, C. Gu and Y. Li, *Anal. Bioanal. Chem.*, 2012, **402**, 687-691.
250. C. Onogi and H. Hamaguchi, *J. Phys. Chem. B*, 2009, **113**, 10942-10945.
- 120 251. L.-d. Chiu, F. Hullin-Matsuda, T. Kobayashi, H. Torii and H.-o. Hamaguchi, *J. Biophotonics*, 2012, **5**, 724-728.
252. B. Davidson, N. Spears, A. Murray and A. Elfick, *J. Raman Spectrosc.*, 2012, **43**, 24-31.
- 125 253. A. G. Shen, J. Peng, Q. H. Zhao, L. Su, X. H. Wang, J. M. Hu and Q. Yang, *Laser Phys. Lett.*, 2012, **9**, 322-328.
254. R. S. Suh, X. Zhu, N. Phadke, D. A. Ohl, S. Takayama and G. D. Smith, *Hum. Reprod.*, 2006, **21**, 477-483.
255. G. Smith, J. Swain and C. Bormann, Seminars in reproductive medicine, 2011.
- 130 256. I. K. Glasgow, H. C. Zeringue, D. J. Beebe, S. J. Choi, J. T. Lyman, N. G. Chan and M. B. Wheeler, *Biomedical Engineering, IEEE Transactions on*, 2001, **48**, 570-578.
257. L. M. Cabrera, G. D. Smith and S. Takayama, *Lab Chip*, 2012, **12**, 2240-2246.
- 135 258. E. Widjaja and M. Garland, *J. Raman Spectrosc.*, 2012, **43**, 828-833.
259. J. Yue, J. C. Schouten and T. A. Nijhuis, *Ind. Eng. Chem. Res.*, 2012, **51**, 14583-14609.

260. P. Rosch, M. Harz, M. Schmitt and J. Popp, *J. Raman Spectrosc.*, 2005, **36**, 377-379.
261. T. Vankeirsbilck, A. Vercauteren, W. Baeyens, G. Van der Weken, F. Verpoort, G. Vergote and J. P. Remon, *TrAC, Trends Anal. Chem.*, 2002, **21**, 869-877.
262. S. Wartewig and R. H. H. Neubert, *Adv. Drug Delivery Rev.*, 2005, **57**, 1144-1170.
263. M. U. Kopp, A. J. De Mello and A. Manz, *Science*, 1998, **280**, 1046-1048.
264. M. C. Ruiz-Martinez, J. Berka, A. Belenkii, F. Foret, A. W. Miller and B. L. Karger, *Anal. Chem.*, 1993, **65**, 2851-2858.
265. D. Xiang, C. Zhang, L. Chen, X. Ji and Z. He, *Analyst*, 2012, **137**, 5898-5905.
266. V. Sikirzhyski, A. Sikirzhyskaya and I. K. Lednev, *Forensic Sci. Int.*, 2012, **222**, 259-265.
267. W. R. Premasiri, J. Lee and L. D. Ziegler, *J. Phys. Chem. B*, 2012, **116**, 9376-9386.
268. A. Sikirzhyskaya, V. Sikirzhyski and I. K. Lednev, *Forensic Sci. Int.*, 2012, **216**, 44-48.
269. M. A. Miller, M. R. Cavaliere, M. Zhou and P. Few, *Spectroscopy*, 2012, **2**, 1-3.
270. K. Faulds and W. E. Smith, in *Infra. Raman Spec. For. Sci.*, eds. J. M. Chalmers, H. G. M. Edwards and M. D. Hargreaves, John Wiley & Sons, Ltd, Chichester, UK., 2012, vol. 6c, pp. 357-366.
271. F. Rull, A. C. Prieto, J. M. Casado, F. Sobron and H. G. M. Edwards, *J. Raman Spectrosc.*, 1993, **24**, 545-550.
272. H. G. M. Edwards, D. W. Farwell, A. C. Williams, B. W. Barry and F. Rull, *Journal of the Chemical Society, Faraday Transactions*, 1995, **91**, 3883-3887.
273. F. B. Baker and L. J. Hubert, *J. Am. Stat. Assoc.*, 1975, **70**, 31-38.
274. K. E. Stephen, D. Homrighausen, G. DePalma, C. H. Nakatsu and J. Irudayaraj, *Analyst*, 2012, **137**, 4280-4286.
275. A.-K. Kniggendorf, T. W. Gaul and M. Meinhardt-Wollweber, *Appl. Spectrosc.*, 2011, **65**, 165-173.
276. M.-L. O'Connell, T. Howley, A. G. Ryder, M. N. Leger and M. G. Madden, *Opto-Ireland 2005: Optical Sensing and Spectroscopy, Ireland*, 2005.
277. G. Deinum, D. Rodriguez, T. J. Romer, M. Fitzmaurice, J. R. Kramer and M. S. Feld, *Appl. Spectrosc.*, 1999, **53**, 938-942.
278. A. S. Haka, K. E. Shafer-Peltier, M. Fitzmaurice, J. Crowe, R. R. Dasari and M. S. Feld, *PNAS*, 2005, **102**, 12371-12376.
279. C. Frausto-Reyes, C. Medina-Gutiérrez, R. Sato-Berrú and L. R. Sahagún, *Spectrochim. Acta, Part A*, 2005, **61**, 2657-2662.
280. M. Berman, A. Phatak, R. Lagerstrom and B. R. Wood, *J. Chemom.*, 2009, **23**, 101-116.
281. G. Gouadec and P. Colomban, *Prog. Cryst. Growth Charact. Mater.*, 2007, **53**, 1-56.
282. A. M. Mouazen, B. Kuang, J. De Baerdemaeker and H. Ramon, *Geoderma*, 2010, **158**, 23-31.
283. I. Pócsik and M. Koós, *Solid State Commun.*, 1990, **74**, 1253-1256.
284. A. Tamura, K. Higeta and T. Ichinokawa, *J. Phys. C: Solid State Phys.*, 1982, **15**, 4975.
285. M. Ferrari, F. Gonella, M. Montagna and C. Tosello, *J. Raman Spectrosc.*, 1996, **27**, 793-797.
286. M. Yoshikawa, Y. Mori, H. Obata, M. Maegawa, G. Katagiri, H. Ishida and A. Ishitani, *Appl. Phys. Lett.*, 1995, **67**, 694-696.
287. M. Yoshikawa, Y. Mori, M. Maegawa, G. Katagiri, H. Ishida and A. Ishitani, *Appl. Phys. Lett.*, 1993, **62**, 3114-3116.
288. S. Sriram, M. Bhaskaran, S. Chen, S. Jayawardhana, P. R. Stoddart, J. Z. Liu, N. V. Medhekar, K. Kalantar-zadeh and A. Mitchell, *J. Am. Chem. Soc.*, 2012, **134**, 4646-4653.
289. Z.-P. Chen, L.-M. Li, J.-W. Jin, A. Nordon, D. Littlejohn, J. Yang, J. Zhang and R.-Q. Yu, *Anal. Chem.*, 2012, **84**, 4088-4094.
290. J. D. Schuttlefield and V. H. Grassian, *J. Chem. Educ.*, 2008, **85**, 279.
291. K. L. A. Chan, S. Gulati, J. B. Edel, A. J. de Mello and S. G. Kazarian, *Lab Chip*, 2009, **9**, 2909-2913.
292. F. Van de Voort, J. Sedman, R. Cocciardi and D. Pinchuk, *Tribol. Trans.*, 2006, **49**, 410-418.
293. C. P. Marshall, E. J. Javaux, A. H. Knoll and M. R. Walter, *Precambrian Res.*, 2005, **138**, 208-224.
294. J. Zięba-Palus and M. Kunicki, *Forensic Sci. Int.*, 2006, **158**, 164-172.
295. C. Krafft, G. Steiner, C. Beileites and R. Salzer, *J. Biophotonics*, 2009, **2**, 13-28.